Chemical Science

ROYAL SOCIETY OF CHEMISTRY

REVIEW

View Article Online
View Journal | View Issue

Cite this: *Chem. Sci.*, 2026, **17**, 1534

Metal-free radical borylations: mechanisms, catalytic strategies, and synthetic applications

Ziyi Quan,[a] Yaxu Liu,[a] Qidi Zhong*[b] and Bo Wang *[a]

Metal-free radical borylation has emerged as a powerful and sustainable alternative to transition-metal-catalyzed methods, addressing challenges such as residual metal contamination, functional group sensitivity, and the high cost of precious metals. This review provides a comprehensive analysis of the mechanistic underpinnings and catalytic innovations driving this rapidly evolving field. We delve into the fundamental steps of radical generation, including homolytic B–X bond cleavage and the formation of alkyl, aryl, and boryl radicals through single-electron transfer (SET), hydrogen atom transfer (HAT), and energy transfer (EnT) pathways. Recent strategic developments are critically evaluated, including photoinduced processes such as electron donor–acceptor (EDA) complex activation, consecutive photoinduced electron transfer (ConPET), and polarity reversal catalysis and electrochemical activation using organic mediators and thermal initiation *via* radical chain processes. Unlike previous reviews, we place a special emphasis on catalytic strategies, substrate scope limitations, and emerging approaches for achieving regiocontrol. The synthetic utility of metal-free radical borylation is highlighted through its application in the late-stage functionalization of pharmaceuticals, natural products, and other complex molecules, enabling transformations that are often difficult to achieve using traditional methods. Finally, we outline the key challenges that continue to shape the field, including selective borylation of unactivated C(sp^3)–H bonds and the scalability of photochemical and electrochemical systems, while also identifying promising future directions in enhancing atom economy, deepening mechanistic understanding, and integrating method development with cutting-edge technology such as high-throughput screening and machine learning. By bridging fundamental radical principles with practical synthesis, this review aims to serve as a roadmap for the continued development of metal-free boron chemistry.

Received 28th October 2025
Accepted 9th December 2025

DOI: 10.1039/d5sc08322b

rsc.li/chemical-science

1. Introduction

Organoboron compounds are among the most versatile and widely utilized intermediates in modern synthetic chemistry, with applications across pharmaceuticals, agrochemicals, and advanced materials (Scheme 1).[1–4] Their utility is exemplified by the Suzuki–Miyaura cross-coupling reaction, a Nobel Prize-winning transformation that relies on boronic acids and esters as key coupling partners.[5] Beyond traditional cross-coupling chemistry, organoboron derivatives play increasingly important roles in emerging areas such as proteolysis-targeting chimeras (PROTACs), fluorogenic probes, and boron neutron capture therapy (BNCT) for cancer treatment.[6–8] The unique electronic and structural features of boron, including its vacant p-orbital and capacity for reversible covalent bonding, underpin a diverse array of reactivity, ranging from 1,2-metallate rearrangements and Petasis reactions to transmetalation processes.[9–11] Consequently, the development of efficient and broadly applicable methods for constructing organoboron compounds remains a central objective in synthetic chemistry.

Over the past few decades, transition-metal-catalyzed borylation reactions, such as Miyaura borylation catalyzed by Pd[12,13] or Ni[14,15] and Ir-catalyzed C–H borylation,[16,17] have served as foundational methods for the synthesis of organoboron compounds. Despite their broad utility, these strategies present several notable limitations. First, concerns regarding toxicity and environmental impact are significant; precious metals such as Pd, Rh, and Ir are costly and generate challenging waste streams and can contaminate products, necessitating rigorous purification in pharmaceutical contexts.[18–20] Second, functional group compatibility remains a recurrent issue, as many metal-catalyzed systems are incompatible with highly reducing or oxidizing groups, certain halides, or acidic protons, thereby restricting substrate scope.[21] Third, these catalytic platforms are frequently sensitive to moisture, oxygen, and ligand degradation, often resulting in diminished yields or catalyst deactivation.[22–25] Finally, the economic and

[a]*Department of Biological Engineering, College of Chemical and Biological Engineering, Shandong University of Science and Technology, Qingdao 266590, PR China. E-mail: wb@sdust.edu.cn*

[b]*School of Pharmacy, North China University of Science and Technology, Tangshan 063009, PR China*

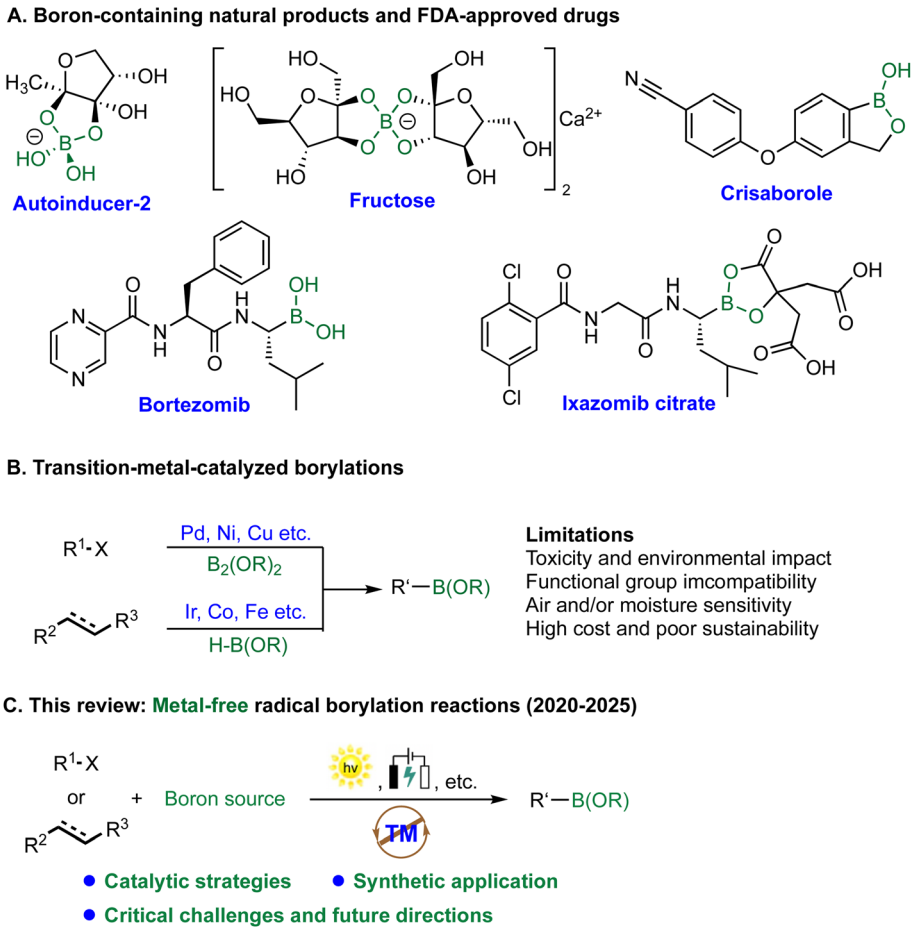

Scheme 1 The importance of organoborons and their synthetic approaches; (A) boron-containing natural products and drugs; (B) transition-metal-catalyzed borylations and their limitations; (C) this review: metal-free radical borylation reactions.

sustainability burdens associated with rare and expensive metals limit the practicality of these methods, particularly in large-scale industrial settings.[26] Although advances in ligand design, including Buchwald-type phosphines[27] and N-heterocyclic carbenes,[28] have mitigated some issues, these solutions often introduce additional complexity and cost. These challenges collectively underscore the growing need for metal-free borylation strategies that preserve the efficiency of traditional metal-catalyzed methods while offering improved sustainability and functional group tolerance.

In recent years, radical borylation reactions have emerged as a powerful complement to traditional metal-catalyzed approaches. By leveraging photochemical, electrochemical, or thermal activation, these methods enable the direct generation of alkyl/aryl/boryl radicals without the involvement of metal intermediates. Metal-free radical borylation offers advantages, including mild and tunable conditions, broad functional group compatibility, and improved sustainability. Significant advances in this area include photoinduced borylation of aryl halides, electrochemical borylation of arenes, and radical-chain processes for alkyl boronate synthesis. While elegant reviews on transition-metal-free borylations have been published,[29–32] a systematic understanding of the mechanistic nuances, catalytic cycles, and substrate limitations remains underdeveloped—a gap this review aims to address.

This review provides a comprehensive analysis of recent advances in metal-free radical borylation reactions (2020–2025), with a particular focus on mechanistic foundations, catalytic strategies, synthetic applications, and critical challenges alongside future directions. By bridging mechanistic understanding with synthetic utility, it not only consolidates current progress but also highlights opportunities for further innovation. We further underscore how metal-free radical borylation can complement and, in some cases, surpass conventional metal-catalyzed approaches, offering a sustainable and versatile toolkit for modern synthetic chemistry.

2. Mechanistic foundation for generation of alkyl/aryl/boryl radicals

The success of metal-free radical borylation reactions hinges critically on the efficient and selective generation of reactive radical species, including alkyl, aryl, and boryl radicals, under mild conditions.[26] A thorough understanding of the mechanisms underlying radical formation provides a conceptual framework for

rational reaction design and the development of new catalytic strategies.

2.1 Generation of alkyl and aryl radicals

In metal-free systems, alkyl and aryl radicals are typically generated *via* electrochemistry, single-electron transfer (SET) or homolytic bond cleavage, initiated by organic photoredox catalysts, electron donors, or heat (Scheme 2A).[33–37] Common precursors for radical generation include alkyl/aryl halides, diazonium salts, redox-active esters (RAEs), sulfonyl derivatives, and quaternary ammonium salts. For instance, metal-free photoexcited catalytic systems can reduce alkyl halides[38–41] or diazonium salts[42–44] to their corresponding radicals *via* an outer-sphere SET mechanism. Thermal initiation with radical initiators, such as diazo compounds and peroxides, promotes the homolytic cleavage of weak bonds to generate alkyl or aryl radicals.[45–47] The nature of the radical precursor profoundly influences the reactivity, lifetime, and selectivity of the radical intermediate, a principle exemplified by stabilized radicals like benzylic and α-heteroatom species, whose enhanced persistence enables broader utility in organic synthesis.[48]

2.2 Generation of boryl radicals

Boryl radicals, which serve as key intermediates in radical borylation, can be generated through several metal-free pathways, typically invoked to arise from homolytic cleavage of B–H or B–B bonds in precursors such as NHC–BH_3, H_3B-base adducts, and diboron reagents (Scheme 2B).[49–51] One of the most established approaches involves photoinduced homolysis of electron-rich boron species under UV or visible light, especially in the presence of suitable hydrogen atom acceptors or radical initiators.[52,53] A representative example is the work of Cao and co-workers, who achieved visible-light-induced Minisci-type borylation of imidazo[1,2-*a*]pyridines with NHC–BH_3. The key NHC-boryl radical intermediate is formed by H-atom abstraction from the borane, followed by fragmentation.[54] Alternatively, transient boryl radicals can be furnished through the single-electron oxidation or reduction of diboron compounds, a process mediated by organophotocatalysts or Lewis base additives that facilitate B–B bond cleavage *via* SET or nucleophile-induced activation.[55,56] Although these pathways are widely cited, direct experimental evidence for boryl radical formation *via* B–H or B–B bond homolysis remains limited. As a result, the involvement of boryl radicals in many systems is often inferred rather than conclusively established, underscoring the need for more definitive mechanistic studies.

2.3 Interplay between radical species

In radical borylation reactions, a key mechanistic element is the selective cross-coupling between carbon-centered (alkyl or aryl) radicals and boryl radicals. The persistent radical effect (PRE) often governs this process, wherein the longer-lived boryl radical selectively traps the transient C-centered radical to forge the desired C–B bond.[57,58] Wang and co-workers developed a radical borylation method using NHC–BH_3 complexes to synthesize organoborons. Mechanistic studies, including cyclic voltammetry and radical clock experiments, confirmed the oxidative generation of NHC-boryl radicals *via* single-electron transfer. Subsequent density functional theory (DFT) calculations explained the observed regioselectivity, revealing a lower activation barrier for addition at the less sterically hindered α-carbon ($\Delta G^{\ddagger}$ = +6.3 kcal mol^{-1}) compared to the β-carbon ($\Delta G^{\ddagger}$ = +14.3 kcal mol^{-1}).[59] These results collectively support a mechanism where NHC-boryl radicals cross-couple with carbon-centered radicals to form products.[59] The PRE is a kinetic phenomenon where a larger difference in lifetime between persistent and transient radicals facilitates a faster and more selective cross-coupling reaction.[57] However, a systematic understanding of boryl radical lifetimes remains elusive, especially when contrasted with the well-established stability trends of carbon-centered radicals.[57,60] Filling this critical gap is

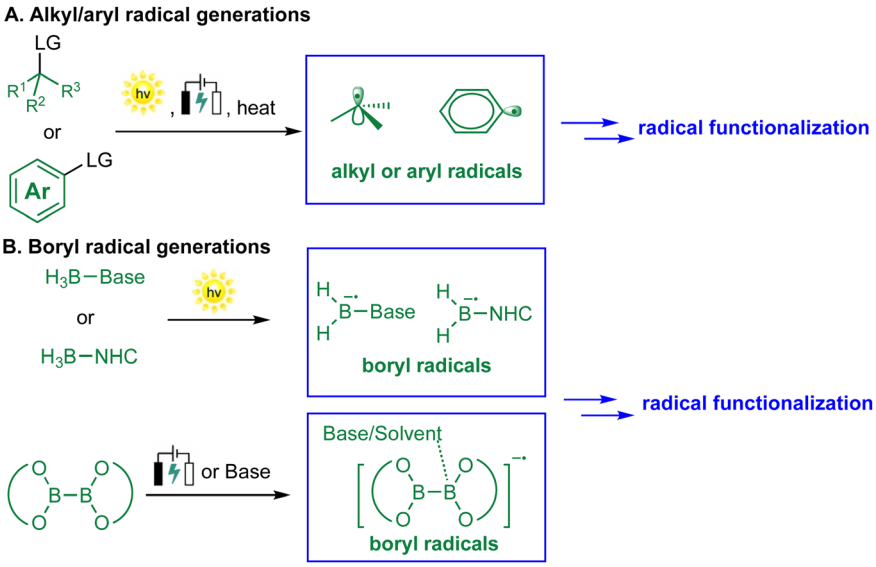

Scheme 2 Approaches for radical generations; (A) alkyl/aryl radical generations; (B) boryl radical generations.

a compelling challenge for the field, one that would fundamentally advance our understanding of their cross-coupling behavior.

3. Catalytic strategies for metal-free radical borylations

3.1 Photoinduced radical borylations

In recent years, photoinduced strategies have emerged as powerful and environmentally benign tools for radical borylation, enabling the generation of reactive radical intermediates under mild conditions without the need for transition metals. Visible light can be harnessed to drive single-electron or energy transfer processes that selectively activate radical precursors or boron reagents. These photoinduced transformations exhibit broad substrate scope, good functional group compatibility, and high synthetic modularity, making them especially attractive for late-stage functionalization and complex molecule synthesis.[26,61]

Within this growing field, four principal mechanistic paradigms have dominated the development of photoinduced radical borylation: single electron transfer (SET), wherein a photocatalyst or excited molecule donates or accepts one electron from a substrate; electron donor–acceptor (EDA) complex activation, which relies on ground-state charge-transfer interactions between substrates; hydrogen atom transfer (HAT), which enables selective C–H bond activation *via* radical relay; and energy transfer (EnT), where triplet excitation leads to radical formation through homolytic cleavage. Each of these strategies offers distinct reactivity profiles and mechanistic advantages, and their application has led to a diverse array of metal-free borylation protocols. In the following subsections, representative examples and mechanistic insights for each mode of these photoinduced radical generations are discussed.

3.1.1 Photoinduced radical borylations *via* SET. Photoinduced SET strategies have become a central platform for radical borylation, enabling the direct conversion of abundant functional groups, including aryl/alkyl halides, redox-active esters, alcohol derivatives, activated C–F bonds, and even unactivated C–H sites, into boronic esters under mild conditions.[26,62,63] These methods benefit from visible-light activation, broad functional-group tolerance, and tunable redox windows offered by photoredox catalysts or organic dyes.[26,62] Common reagents include diboron sources such as B_2pin_2 and B_2cat_2; Lewis bases or alkoxide activators that generate reactive boron 'ate' complexes; and sacrificial electron donors such as amines, thiolates, or Hantzsch esters. Depending on the activation mode, additional additives such as bases, thiols, or HAT mediators (*e.g.*, benzophenone derivatives and polyoxometalates) guide radical generation and control selectivity.[26,63] Collectively, these tools expand disconnection strategies beyond traditional two-electron approaches and provide streamlined access to synthetically versatile boronates.

Despite these advantages, photoinduced SET borylations face several recurring constraints. Oxygen sensitivity remains

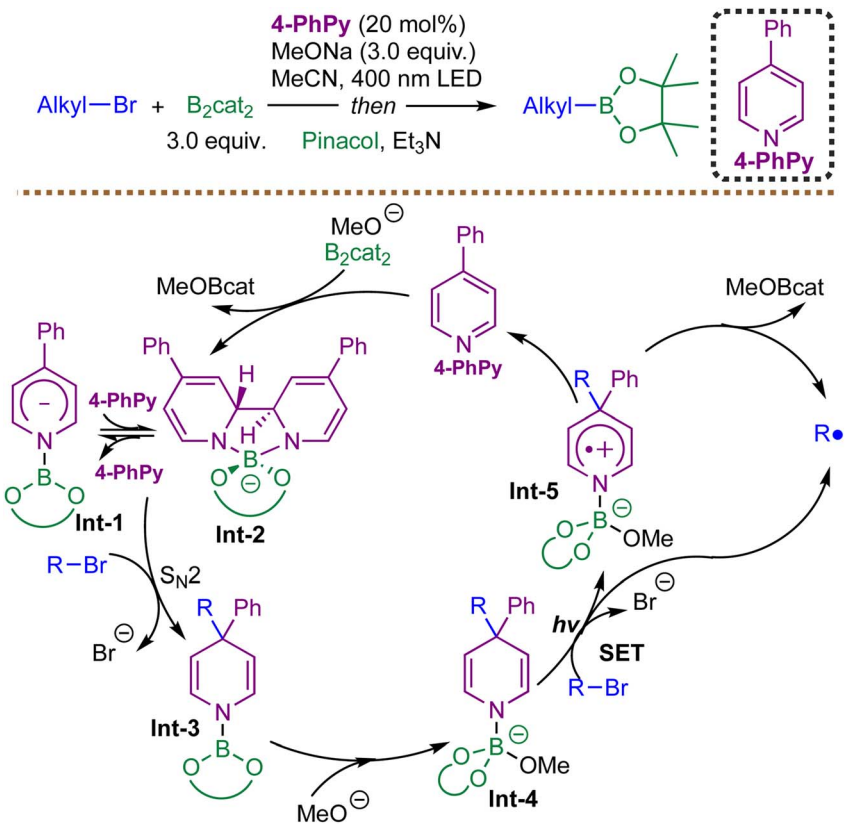

Scheme 3 Photoinduced radical borylations catalyzed by 4-phenylpyridine.

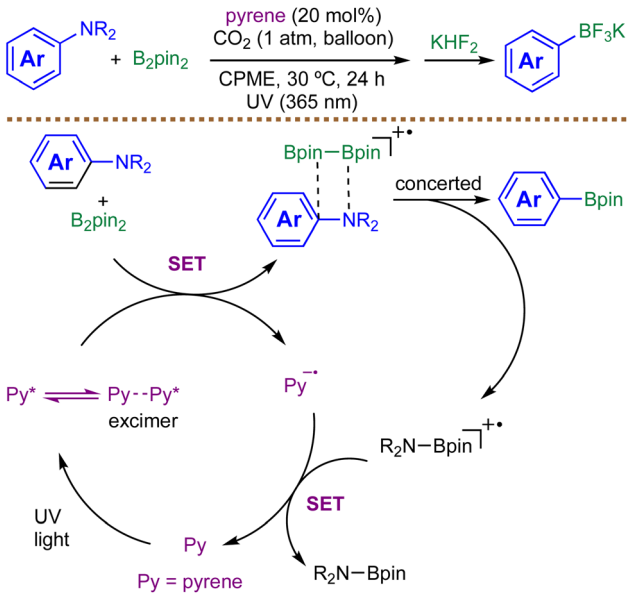

Scheme 4 Photoinduced deaminative borylations enhanced by CO_2.

a major operational challenge, and successful transformations require careful matching of excited-state redox potentials with substrate reduction thresholds—factors that limit the activation of strongly electron-rich arenes or robust C–X bonds.[64,65] Radical pathways can suffer from competing β-scission, protodehalogenation, or regioselectivity issues, especially in HAT-based protocols.[65–67] Moreover, key mechanistic questions persist, including the precise origin and nature of the active boryl species, the role of Lewis bases in modulating the B–B bond activation landscape, and whether reactions proceed through discrete boryl radicals, boronate radical anions, or mixed chain–photocatalytic manifolds.[66] Clarifying these mechanistic ambiguities will be essential for rational catalyst design and for overcoming current redox and substrate-scope limitations in future SET-driven borylation chemistry.

Building on the growing interest in organocatalytic radical borylation, Jiao *et al.* reported in 2020 an efficient visible-light-induced, transition-metal-free radical borylation of unactivated alkyl bromides catalyzed by 4-phenylpyridine.[68] This method leverages a novel nucleophilic substitution/photoinduced radical formation pathway, enabling the conversion of alkyl bromides into alkylboronic esters under mild conditions (Scheme 3).

The reaction exhibits broad substrate scope, accommodating primary, secondary, and even certain tertiary alkyl bromides, with good functional group tolerance. However, its compatibility with (hetero)aryl bromides remains elusive. Mechanistically, the process begins with the formation of electron-rich ate complexes **Int-1** and **Int-2** from 4-phenylpyridine, bis(catecholato)diboron (B_2cat_2), and methoxide. These intermediates act as potent nucleophiles, engaging alkyl bromides in an S_N2 reaction to generate 4-alkyl-1,4-dihydropyridine (DHP) derivative **Int-3**, which is subsequently converted to **Int-4** upon methoxide coordination. Under photoirradiation, **Int-4** undergoes SET to another molecule of alkyl bromide, generating alkyl radicals *via* homolytic C–C bond cleavage of the transient radical intermediate **Int-5**. The resulting alkyl radicals are efficiently trapped by diboron reagents to form alkylboronate. Notably, the reaction does not proceed *via* direct photoinduced SET from the initial ate complex to the alkyl bromide; rather, the nucleophilic substitution step is essential for enabling radical formation. This mechanistic distinction accounts for the method's effectiveness with unactivated alkyl bromides, which are typically resistant to single-electron reduction. The study further demonstrates the versatility of this organocatalytic system in other radical processes, including dehalogenation and cyclization, underscoring its broad synthetic utility. Nevertheless, the method exhibits limitations with more challenging electrophiles; subsequent work by the same group indicates that extending the protocol to unactivated alkyl chlorides remains notably difficult.[69]

Aromatic amines are important feedstocks in organic synthesis. In 2021, Kuninobu and coworkers reported a photoinduced, metal-free borylation of unreactive aromatic amines *via* direct C(sp^2)–N bond cleavage, employing pyrene as an organic photocatalyst under UV irradiation (Scheme 4).[70] GC-MS analysis and radical-trapping experiments with TEMPO and 1,1-diphenylethylene indicate that the transformation does not proceed through α-aminoalkyl radicals, aryl radicals, or aryl cations. These observations suggest that both C–N bond cleavage and C–B bond formation likely occur through a concerted pathway. However, direct experimental evidence for this proposed concerted C–N cleavage/C–B bond-forming event remains lacking, and further mechanistic studies would be valuable for substantiating this hypothesis. A key feature of the protocol is the use of a CO_2 atmosphere, which mitigates inhibition by the byproduct pinB-NMe_2 (detected *via* ^{11}B NMR),

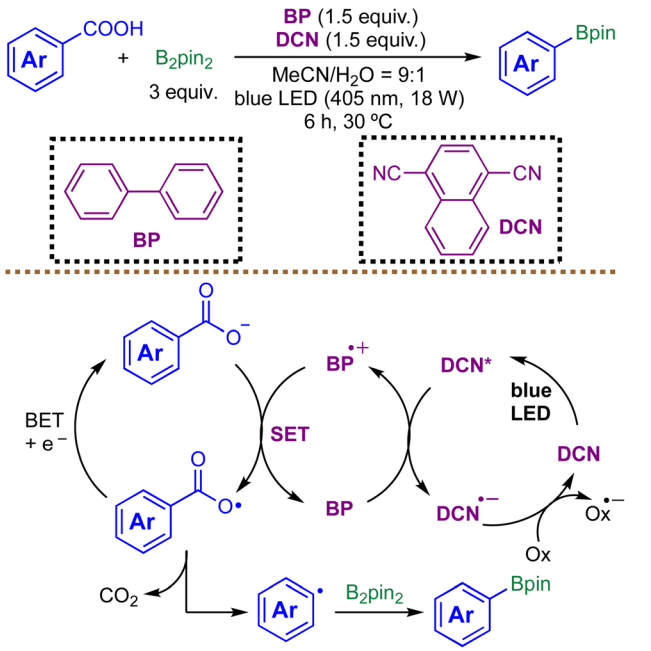

Scheme 5 Photoinduced decarboxylative radical borylation by Yoshimi *et al.*

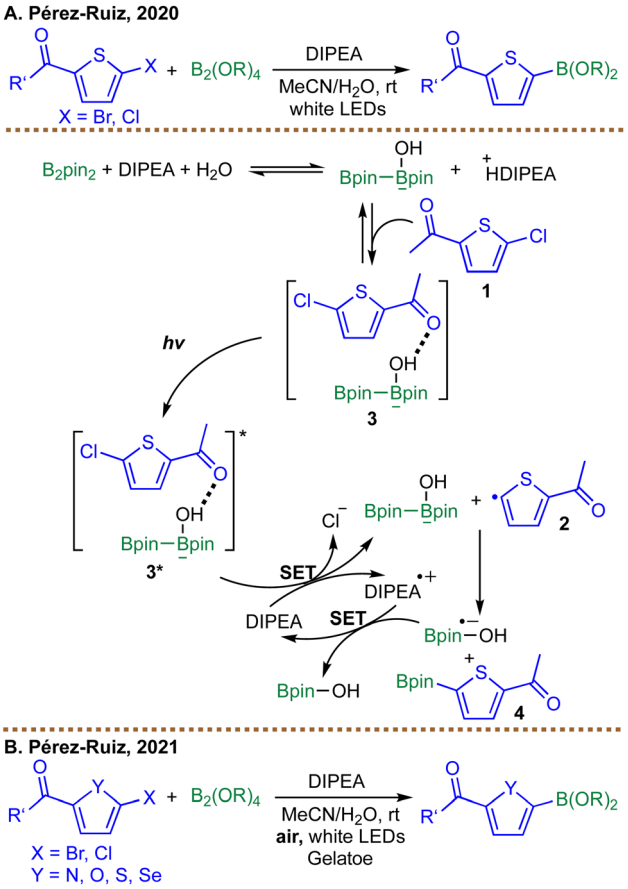

Scheme 6 Visible-light-driven radical borylation by Pérez-Ruiz *et al.*; (A) borylation of thiophenes in 2020; (B) borylation of heteroarenes in 2021.

likely by destabilizing its interaction with reactive intermediates. Mechanistically, photoexcitation of pyrene initiates SET to generate a complex between the arylamino radical cation and bis(pinacolato)diboron (B_2pin_2). Subsequent concerted C–N cleavage and C–B bond formation generates the desired boronic ester product along with an aminoboryl radical cation, which then undergoes SET with the pyrene radical anion to form aminoborane and regenerate pyrene. The protocol demonstrates tolerance for a range of functional groups, including silyl, esters, and methoxy, and affords the desired products in moderate to good yields. Its applicability is nonetheless limited by steric hindrance, as ortho-substituted substrates provide significantly diminished yields or no reaction. This work represents a pioneering example of direct C–N borylation without preactivation or metal catalysis, expanding the toolbox for arylboronic ester synthesis.

While aryl radicals are valuable reactive intermediates, they are generally less stable than alkyl radicals. Traditional formation of aryl radicals involves harsh reactions, stoichiometric amounts of toxic metals (Sn and Ag), or explosive reagents such as diazonium salts. Yoshimi *et al.* introduced a photoinduced decarboxylative radical borylation reaction of benzoic acids using an organic photoredox catalyst system consisting of biphenyl (BP) and 1,4-dicyanonaphthalene (DCN) in 2020 (Scheme 5).[71] The mechanism involves photoinduced SET from BP to DCN under light irradiation, generating a BP radical cation and a DCN radical anion. The BP radical cation oxidizes the benzoate ion to form an aryl carboxy radical, which undergoes decarboxylation upon mild heating to yield an aryl radical. This aryl radical then reacts with B_2pin_2 to form arylboronate esters.

The decarboxylation of benzoic acids is particularly challenging because aryl carboxy radicals decarboxylate more slowly than their alkyl counterparts. While conventional photocatalysts like $Ir(ppy)_3$ and $Ir[dF(CF_3)ppy]_2(dtbbpy)^+$ fail to

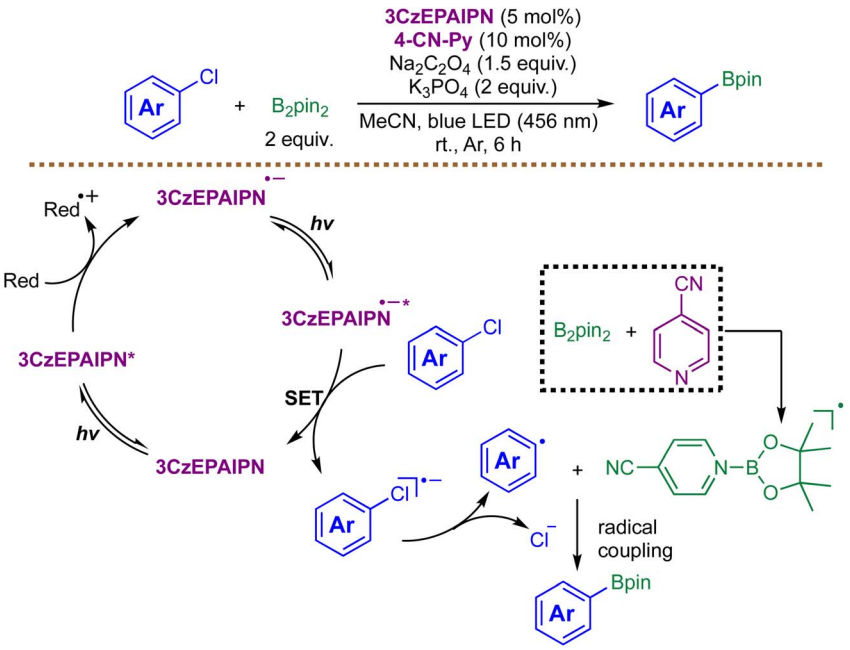

Scheme 7 Borylation of aryl chlorides through the ConPET process.

promote this reaction, the BP/DCN system achieves it successfully, underscoring its unique reactivity profile.[71] Nevertheless, the authors report only 12 radical borylation examples, predominantly limited to simple aryl substrates. As a result, the reactivity of this method toward aliphatic, heteroaryl, or sterically hindered substrates remains largely unexplored.

In the same year, Pérez-Ruiz *et al.* reported a visible-light-driven, photocatalyst-free borylation of thiophenes using B_2pin_2 with DIPEA as the base (Scheme 6A).[72] The reaction proceeds *via* the formation of a ground-state complex **3** between the thiophene substrate **1**, B_2pin_2, and DIPEA, which absorbs visible light to initiate the transformation. Upon irradiation, the excited complex **3*** undergoes SET to generate a thiophene radical intermediate **2**, as confirmed by trapping experiments with PhSSPh. This radical subsequently reacts with B_2pin_2 to yield the borylated product **4**, while DIPEA acts as both a proton acceptor and an electron donor to close the catalytic cycle.

The study highlights the role of non-covalent interactions, particularly hydrogen bonding between the thiophene carbonyl group and the diboron-base adduct, in facilitating the reaction. A limitation of this approach is its sensitivity to oxygen, necessitating anaerobic conditions. To overcome this, their follow-up work introduced a supramolecular gel nanoreactor to enable aerobic borylation (Scheme 6B).[73] The gel confined the reaction microenvironment, protecting radical intermediates from oxygen quenching while the same ground-state complex (substrate/B_2pin_2/DIPEA) absorbed visible light to initiate the reaction. The gel's fibrillar network suppresses parasitic pathways, such as singlet oxygen formation, enabling efficient borylation of diverse heteroarenes in air. The substrate scope is largely restricted to five-membered, electron-rich heteroarenes, such as furan, thiophene, selenophene, and pyrrole derivatives. Notably, the manuscript does not include examples of six-membered heteroaromatics (*e.g.*, pyridines and quinolines) or simple (hetero)aryl substrates, leaving the applicability of the protocol to these more common motifs uncertain.

While Pérez-Ruiz's method demonstrated the potential of photocatalyst-free borylation, its reliance on specific substrate interactions and sensitivity to oxygen posed limitations. A more general and powerful approach was introduced in 2021 by Wu and coworkers, who demonstrated a groundbreaking advancement in metal-free radical borylation through a consecutive photoinduced electron transfer (ConPET) process (Scheme 7).[74] The authors designed a donor–acceptor cyanoarene-based photocatalyst 3CzEPAIPN, which undergoes a two-photon excitation mechanism to achieve extreme reduction potentials (up to −2.94 V *vs.* SCE). Mechanistically, the key step is the generation of a long-lived radical anion $3CzEPAIPN^{\bullet-}$ *via* initial photoexcitation. This persistent intermediate absorbs a second photon, forming a highly potent reductant $3CzEPAIPN^{\bullet-}$*

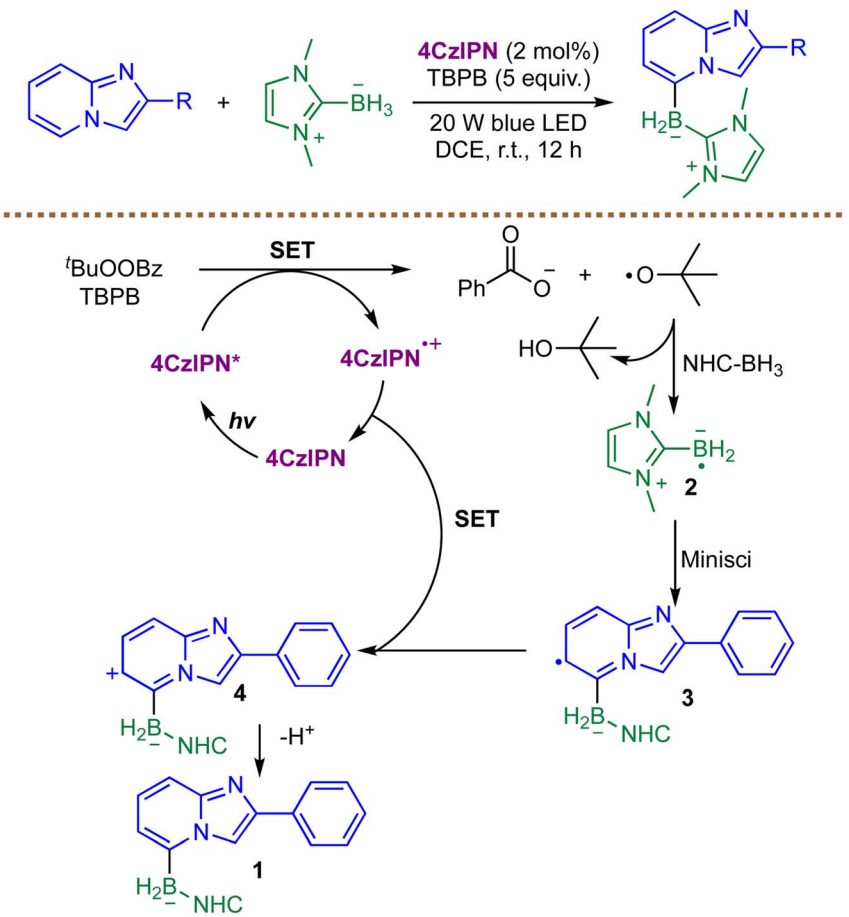

Scheme 8 C-5 selective radical borylation of imidazo[1,2-α]pyridines using NHC–BH_3.

capable of activating even recalcitrant aryl chlorides *via* SET. The resulting aryl radicals then couple with boryl radicals to furnish the arylboronate products. While this method is distinguished by its mild conditions and ability to functionalize a wide range of substrates, including electron-rich and complex pharmaceutical aryl chlorides, it is not without limitations. Competing dechlorination represents a significant side reaction, particularly for substrates bearing hydroxy or methylsilyl groups, and the applicability of the protocol to alkyl chlorides remains unexplored.

Recent advances in the design of boronating reagents have created new opportunities in organoboron synthesis. Of particular note are NHC-boranes, which have garnered considerable attention due to their remarkable thermal stability and multifaceted reactivity.[75,76] A 2022 report by Cao and co-workers reported a visible-light-induced, C-5 selective radical borylation of imidazo[1,2-α]pyridines using NHC–BH_3 as the boryl source (Scheme 8).[77] This work marks an expansion of Minisci-type borylation to electron-rich heteroarenes. The proposed mechanism features a synergistic photocatalytic cycle: upon irradiation, excited 4CzIPN* undergoes a SET with the oxidant *tert*-butyl perbenzoate (TBPB), yielding a *tert*-butoxy radical and the oxidized photocatalyst $4CzIPN^{\bullet+}$. Subsequent hydrogen atom transfer from NHC–BH_3 to the *tert*-butoxy radical generates the crucial NHC-boryl radical **2**, which adds regioselectively to the C-5 position of the protonated substrate. The resulting radical intermediate **3** is then oxidized by $4CzIPN^{\bullet+}$, concurrently regenerating the ground-state photocatalyst and furnishing the borylated product **1** after deprotonation. Mechanism evidence, including radical trapping with TEMPO and BHT, underscores the dual role of the photocatalyst in both initiating the radical chain *via* SET oxidation and terminating the cycle, establishing a robust metal-free strategy for synthesizing heteroaryl boronic esters. However, the method was evaluated exclusively on imidazo[1,2-*a*]pyridine substrates, leaving other (hetero)aryl or non-azine arenes untested. Furthermore, the reported examples are limited to a small set of substituted imidazo[1,2-*a*]pyridines, with little to no demonstration of highly functionalized derivatives, diverse substitution patterns, sterically hindered scaffolds, or heterocycles bearing sensitive functional groups.

Building on the theme of metal-free radical borylation, the strategy was further extended to cascade cyclizations. In 2023, Wei *et al.* described a photoinduced arylboration of unactivated alkenes for the synthesis of indoline boronic esters (Scheme 9).[78] This method leverages visible-light irradiation to generate aryl radicals **8** *via* homolysis of the C–I bond in alkene-tethered aryl iodides. A key feature is a potential chain-propagation step where a boryl radical **10** could reform the aryl radical **8** with aryl iodide **5** *via* SET or the halogen-atom transfer (XAT) process, bypassing the need for a stoichiometric photocatalyst or additives. The mechanism proceeds through an intramolecular cyclization with the unactivated alkene, followed by trapping with B_2cat_2 to yield the boronate product **6**. The reaction proceeds efficiently in DMF, likely due to the stabilization of boryl radicals by the solvent, and does not require additional bases or photosensitizers. Control experiments, including

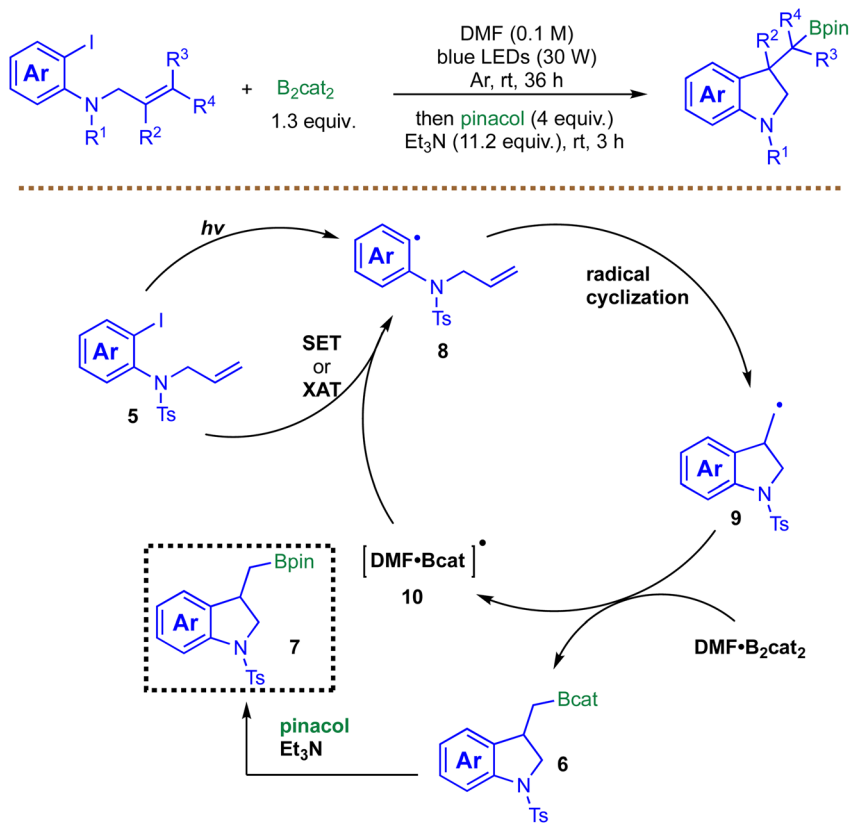

Scheme 9 Photoinduced arylboration of unactivated alkenes by Wei *et al.*

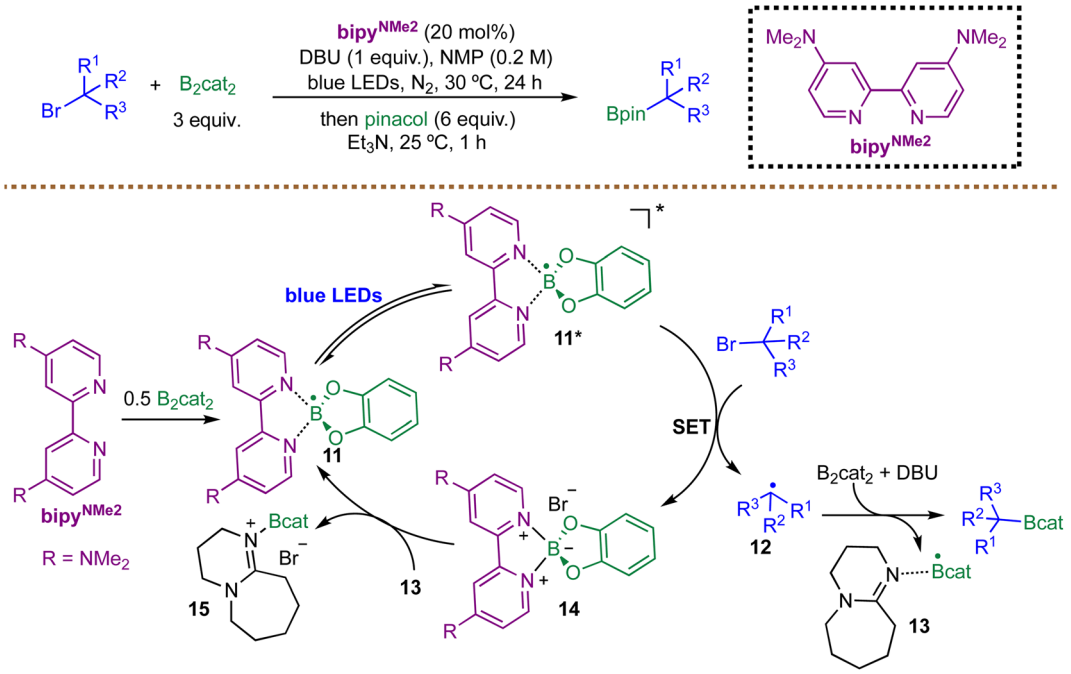

Scheme 10 Photoinduced debrominative borylations.

radical scavenger studies and a radical clock experiment, support a radical-based pathway. The method was demonstrated primarily on alkenes tethered to an amine (phenylamine or alkylamine), while simple unactivated alkenes lacking such tethers remain untested. Moreover, given the limited set of examples, the robustness of the reaction toward sterically hindered alkenes, highly substituted substrates, or alkenes bearing sensitive functional groups remains uncertain.

While persistent boryl radicals are often generated from NHC-boranes, Aggarwal and co-workers recently introduced a transformative concept using a persistent boryl radical derived from a diboron reagent and a bipyridine as a direct photoredox catalyst (Scheme 10).[79] The catalytic species, a boryl-bipyridine radical **11**, is easily prepared *in situ* from bipyridines and B_2cat_2 and exhibits exceptional ground-state stability. Upon photoexcitation with blue light, the boryl-bipyridine radicals **11** form highly reducing doublet excited state **11*** with a reduction potential of −3.46 V *vs.* SCE, rivaling the strongest photoreductant known. The mechanism proceeds *via* SET from the excited-state radical **11*** to the alkyl bromide, generating alkyl radicals **12.** This radical is then trapped by B_2cat_2 in the presence of DBU to form the corresponding boronic esters. Finally, the reduction of **14** by **13** regenerates **11** and **15.** The authors confirmed that the borylbipyridine radical **11** was the active

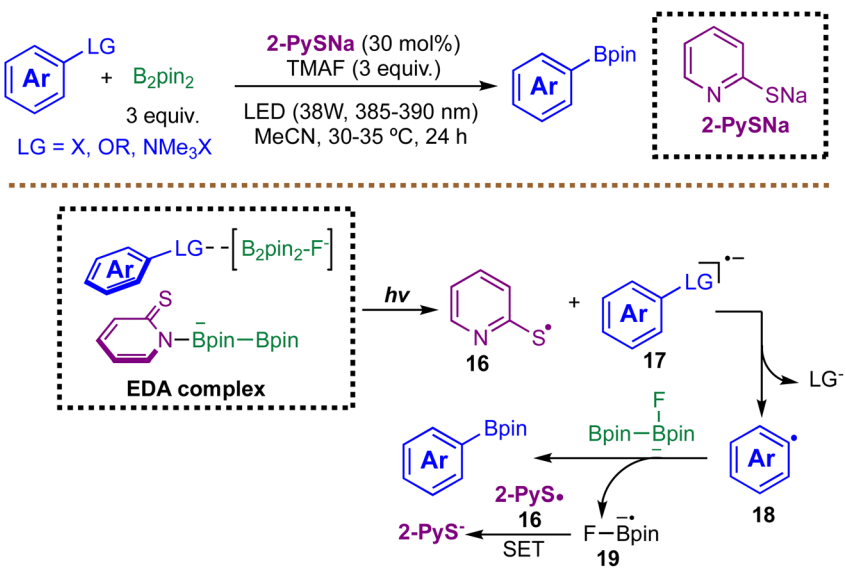

Scheme 11 Photoinduced thiolate catalytic radical borylation.

photocatalytic species in the radical borylation through a combination of techniques, including EPR spectroscopy, NMR studies, and cyclic voltammetry. While the boryl radical catalysts are described as "persistent", the long-term stability and handling of these radical catalysts on a large scale are not thoroughly addressed.

3.1.2 Photoinduced radical borylations *via* EDA complex activation. While the SET pathway, particularly when empowered by potent photoreductants, provides a powerful and general strategy for radical generation, its fundamental reliance on favorable redox thermodynamics presents an inherent limitation. This thermodynamic barrier restricts its application to substrates that fall within the catalyst's redox window, often excluding those with highly negative reduction potentials.[80] To circumvent this constraint, an alternative paradigm that bypasses the need for long-range electron transfer has emerged: radical generation through EDA complex activation.

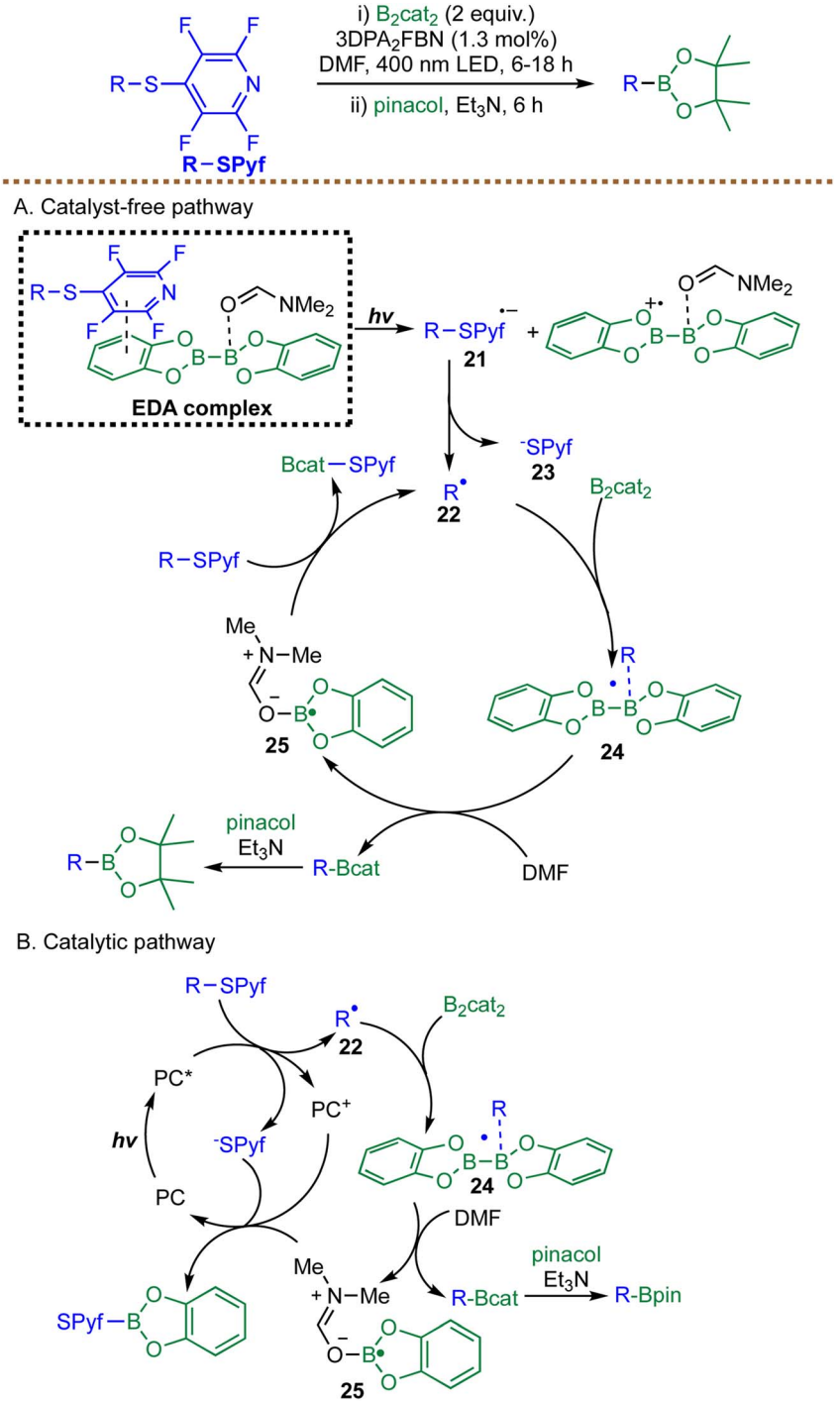

Scheme 12 Light-mediated sulfur–boron exchange.

In contrast to conventional photoredox catalysis where SET proceeds through diffusional encounters between a photocatalyst and substrate, EDA complexes pre-organize the donor (*e.g.*, thiolates and amines) and acceptor (*e.g.*, aryl halides and sulfonates) into a ground-state assembly capable of direct photoactivation.[81] This pre-associated architecture obviates the need for highly reducing photocatalysts, as localized charge-transfer excitation—often accessible under visible-light irradiation—can promote bond cleavage and initiate radical generation.[82] Such features render EDA complex activation a compelling strategy for engaging inert substrates and enabling transformations such as radical borylation under mild conditions. The following section highlights key advances in EDA complex-mediated reactions, where the interplay of donor–acceptor pairing and light absorption unlocks unconventional substrates and mechanistic pathways.

In 2021, König *et al.* reported a thiolate-catalyzed photoredox protocol that enables radical borylation of otherwise inert C(aryl)–X bonds (X = F, O, N, S) under visible-light irradiation (Scheme 11).[83] The transformation proceeds *via* formation of a photoactive EDA complex between the thiolate catalyst (2-PySNa) and the aryl substrate, a process promoted by the in situ–generated boryl anion species $[B_2pin_2–F]^-$ derived from B_2pin_2 and fluoride. Photoexcitation of this EDA complex triggers an inner-sphere electron transfer, furnishing thiyl radical **16** and radical anion **17**. The latter undergoes rapid SET to produce aryl radical **18**, which subsequently reacts with $[B_2pin_2–F]^-$ to deliver the borylated product alongside boryl radical anion **19**. Reduction of thiyl radical **16** by boryl radical anion **19** then regenerates the thiolate catalyst, completing the catalytic cycle. Spectroscopic studies (UV-Vis and NMR) together with radical trapping experiments support the involvement of charge-transfer activation and aryl radical intermediates in the catalytic cycle. The method demonstrates broad substrate scope (>50 examples), accommodating a wide range of leaving groups, including OBoc, SO_2R, and NR_3^+, and diverse functional groups. However, this method is not universally applicable. Sterically congested ortho-substituted substrates (*e.g.*, *o*-phenyl aryl fluorides) often inhibit productive borylation, instead promoting hydrodefluorination or decomposition. Likewise, certain sulfur-containing substrates, such as thioanisole, exhibit poor reactivity, indicating that C–S bond activation is substrate-dependent. In addition, hydrodehalogenation frequently competes with the desired borylation pathway—particularly in the case of phenol derivatives (Ar–OBoc) and sterically encumbered arenes—highlighting a key limitation of the current system.[83]

Building on the growing interest in radical borylation *via* EDA complexation, Dilman and Panferova introduced a complementary approach in the same year, focusing on C(sp^3)–S bond activation using a distinct sulfur-based radical precursor. They reported a novel metal-free strategy for the radical borylation of alkyl sulfides, exploiting the unique reactivity of the tetrafluoropyridinylthio (PyfS) group as a radical precursor (Scheme 12).[84] This method involves irradiating sulfides with B_2cat_2 in DMF, followed by transesterification with pinacol to afford the corresponding pinacol boronic esters. A key mechanistic feature is the highly electron-deficient PyfS group, which facilitates radical initiation. The authors propose

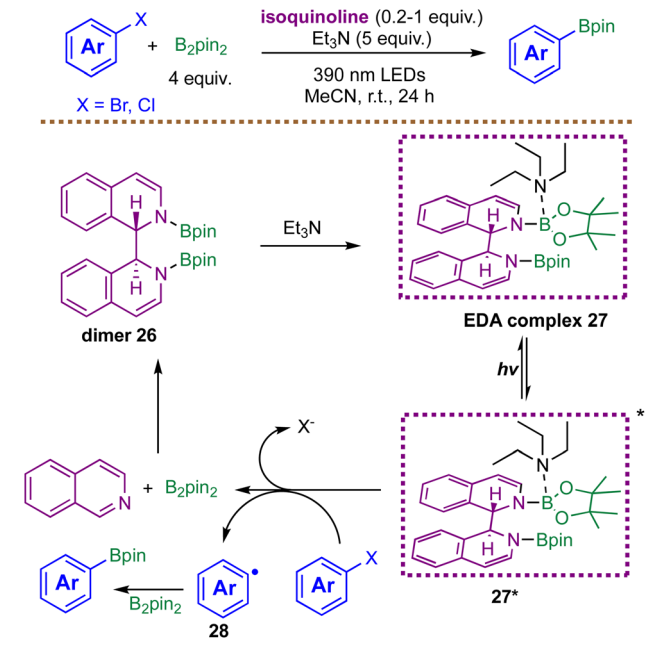

Scheme 13 Photoinduced metal-free borylation of aryl halides.

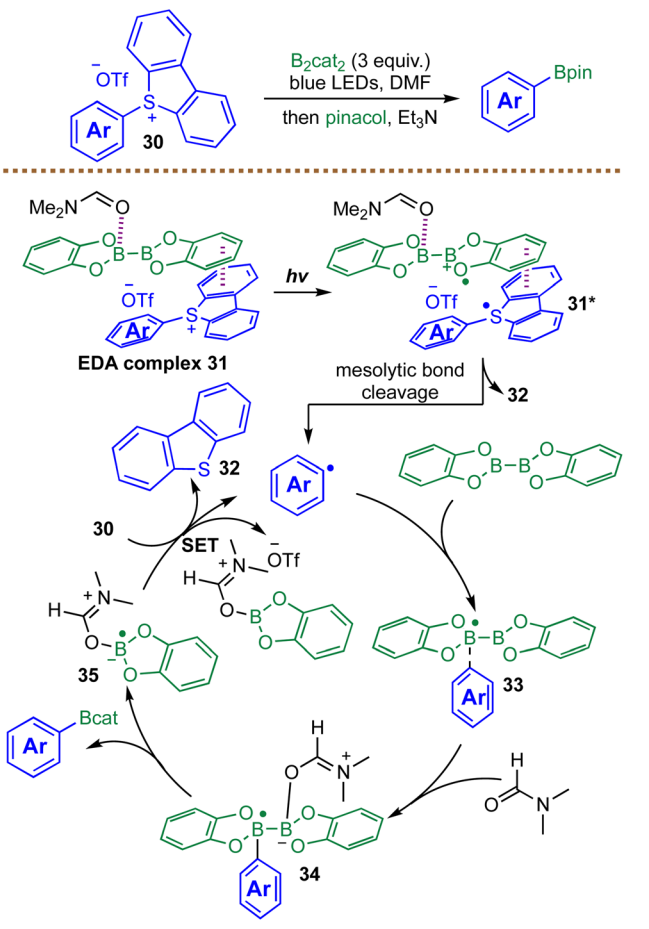

Scheme 14 Borylation of thiophenium salts *via* EDA complexation.

two parallel pathways: a catalyst-free EDA complex mechanism and a photocatalyzed cycle. In the EDA complex pathway, the electron-rich diboron reagent and the electron-poor sulfide form a complex. Upon photoexcitation, SET generates a sulfide radical anion **21**, which fragments to yield an alkyl radical **22** and a PyfS anion **23**. The alkyl radical **22** subsequently attacks B_2cat_2 to form an alkylboryl radical species **24**, which, in the presence of DMF, produces the desired product along with radical species **25**. Radical **25** then acts as a chain carrier, reducing another molecule of sulfide and regenerating alkyl radical **22**. In the alternative catalytic pathway, an organic photocatalyst 3DPA2FBN is oxidatively quenched by the sulfide to generate the same alkyl radical **22**, which then reacts with B_2cat_2. This protocol shows broad applicability, enabling efficient borylation of primary, secondary, and even sterically encumbered tertiary alkyl sulfides. However, the need to pre-install the electron-withdrawing tetrafluoropyridinyl sulfenyl (PyfS) group reduces the overall step economy and adds an extra preparative burden.

Motivated to circumvent the need for pre-functionalized radical precursors, Wang and co-workers in 2022 introduced a complementary metal-free protocol that enables the radical borylation of aryl halides through an *in situ* generated EDA complex (Scheme 13).[85] In their system, isoquinoline, B_2pin_2, and triethylamine form a photoactive assembly in acetonitrile under 390 nm irradiation. Mechanistic and computational studies indicate that the key reducing species is an excited-state EDA complex **27***, derived from a pre-catalyst dimer **26** and NEt_3 as the electron donor. Time-dependent DFT calculations reveal that this photoexcited complex **27*** exhibits an exceptionally negative reduction potential (−3.12 V *vs.* SCE), enabling single-electron reduction of even electron-rich aryl chlorides. The resulting aryl radical **28** is subsequently captured by B_2pin_2 to furnish the corresponding boronic esters. The developed protocol enables the synthesis of arylboronic esters from abundant and readily available aryl chlorides and bromides; however, it requires a superstoichiometric amount of Et_3N to promote efficient radical formation. Taken together, the studies by Dilman[84] and Wang[85] highlight a clear trade-off in EDA-driven radical borylation strategies: protocols employing pre-functionalized radical precursors circumvent the need for bases or superstoichiometric additives, whereas methods that engage unactivated substrates—such as native aryl halides—typically rely on substantial quantities of electron donors or other additives to achieve efficient radical generation.

While Dilman developed a radical borylation strategy for pre-functionalized alkyl sulfides to access alkyl boronic esters,[84] Rueping and co-workers introduced a complementary approach in 2022, accessing aryl boronic esters through a highly para-selective, catalyst-free borylation of aryl dibenzothiophenium salts **30** with B_2cat_2 under blue light irradiation (Scheme 14).[86] Mechanistic investigations, including UV-vis spectroscopy and a radical clock experiment, confirmed the formation of a visible EDA complex **31** between the electron-deficient dibenzothiophenium salts **30** and the electron-rich B_2cat_2. Photoexcitation of this complex **31** triggers a SET from B_2cat_2 to

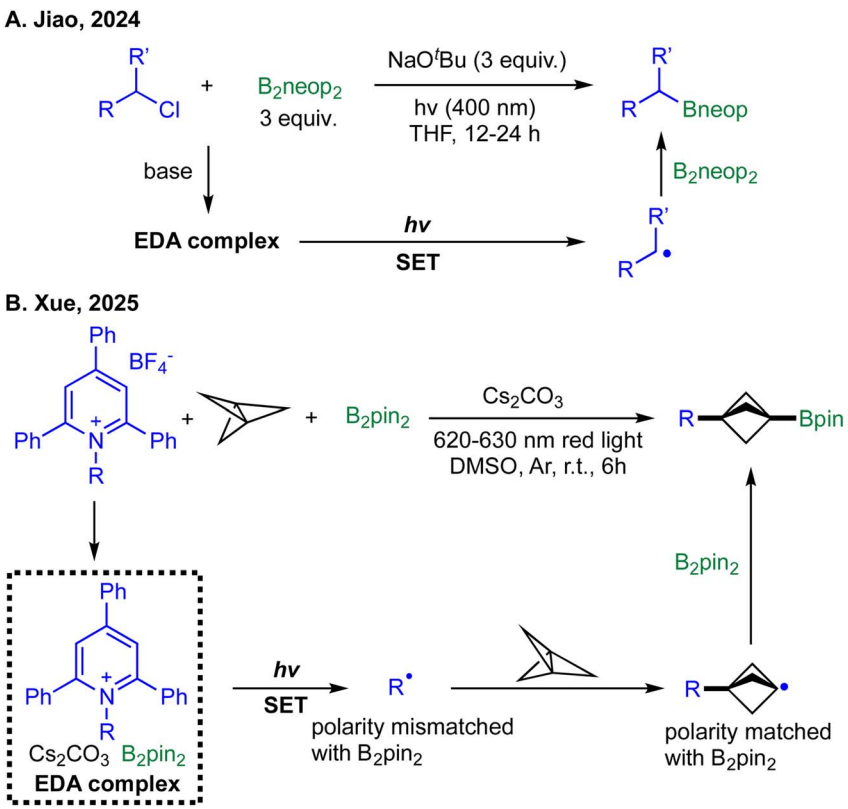

Scheme 15 Photoinduced radical borylation of alkyl chlorides or Katritzky salts.Recent photoinduced radical borylations; (A) borylation of alkyl chlorides by Jiao *et al.* in 2024; (B) borylation of Katritzky salts by Xue *et al.* in 2025.

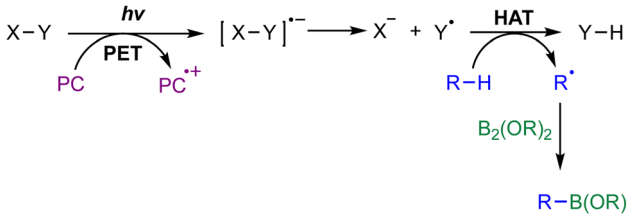

Scheme 16 C–H borylations *via* the HAT pathway.

30, generating the radical anion **31***, which undergoes mesolytic cleavage to release the key aryl radical and recyclable dibenzothiophene **32**. The chain-propagation cycle is proposed to proceed *via* addition of the aryl radical to B_2cat_2, forming a boryl radical intermediate **33**. Subsequent complexation with a molecule of DMF affords a new radical intermediate **34**, which undergoes B–B bond cleavage to furnish the desired aryl boronic ester. The further SET event between intermediate **35** and another molecule of **30** regenerates the aryl radical, closing the catalytic cycle. This elegant mechanism enables the conversion of readily prepared, para-selective dibenzothiophenium salts into valuable aryl boronic esters with good functional-group tolerance and has been successfully applied to the late-stage functionalization of complex natural products and pharmaceuticals. Nevertheless, the reactivity of heteroaryl or alkyl substrates under the developed conditions remains unclear. A gram-scale borylation of a vitamin E-derived substrate was successfully performed under the standard conditions, furnishing the corresponding boronic ester in 52% yield compared to 71% yield on a 0.1 mmol scale, indicating a modest decrease in efficiency upon scale-up.[86]

The most recent advancements in metal-free radical borylation are exemplified by two distinct yet complementary strategies that leverage photoinduced EDA complex formation. In the first approach, Jiao *et al.* demonstrated that unactivated alkyl chlorides can be directly borylated using bis(neopentyl glycolato)diboron (B_2neop_2) and NaO^{t}Bu under 400 nm irradiation, without the need for any photocatalyst (Scheme 15A).[69] Mechanistic studies, including radical-clock experiments and TEMPO trapping, confirmed the formation of alkyl radicals. The authors propose that the critical initiation step involves a photoinduced SET facilitated by an EDA complex formed between B_2neop_2, the alkoxide base, and the alkyl chloride substrate. UV-Vis spectroscopy supported this hypothesis, showing a bathochromic shift upon mixing the components. Upon irradiation, the generated alkyl radicals react with B_2neop_2 to furnish desired alkyl boronic esters. While the protocol performs efficiently with primary and secondary alkyl chlorides, the study does not demonstrate successful borylation of more challenging substrates, such as sterically hindered tertiary chlorides. This limitation narrows the overall generality of the method, particularly when compared with alternative radical-generation strategies such as Dilman's sulfenyl-precursor approach,[84] which tolerates a broader range of substrate classes.

In a mechanistically distinct yet conceptually related advance, Xue *et al.* reported a red-light-induced deaminative borylation of [1.1.1]propellane using Katritzky salts and B_2pin_2 (Scheme 15B).[87] In this ternary system, the combination of the Katritzky salt, B_2pin_2, and Cs_2CO_3 forms a red-light-absorbing EDA complex that undergoes SET to generate nucleophilic alkyl radicals. The ensuing reactivity is governed by polarity matching: the alkyl

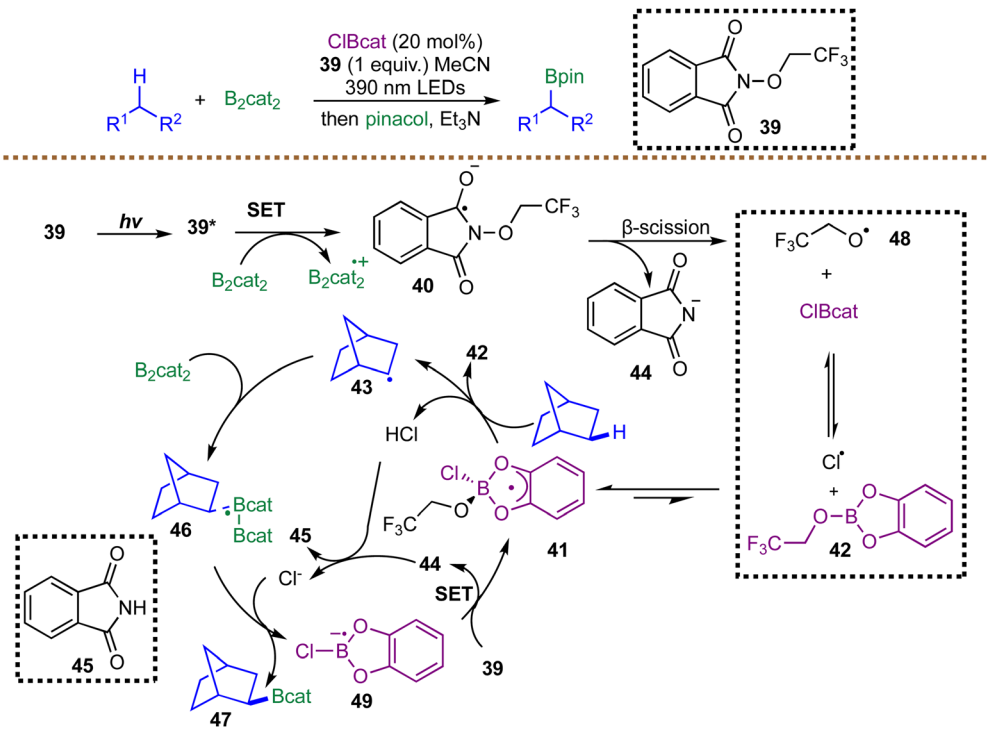

Scheme 17 Metal-free photoinduced C–H borylation of alkenes.

radical first adds to the strained [1.1.1]propellane framework, forming an electrophilic, sp^2-hybridized bridgehead bicyclo[1.1.1]pentyl radical. This intermediate is then selectively trapped by the more electron-rich B_2pin_2, yielding the difunctionalized product. This study showcases a refined application of EDA complex photochemistry, demonstrating how red-light activation and intrinsic electronic bias within radical intermediates can be harnessed to achieve selective multicomponent borylation. The study demonstrates compatibility with a range of alkyl Katritzky salts; however, it does not systematically examine the impact of steric bulk on the radical precursor, such as tertiary, branched, or otherwise bulky substituents, on addition to [1.1.1]propellane and subsequent Bpin trapping. Consequently, the robustness of the method toward sterically demanding alkyl fragments remains uncertain.

3.1.3 Photoinduced radical borylations *via* HAT. While activation of organic substrates through photoinduced EDA complexes has emerged as a powerful metal-free platform for radical generation, the strategy carries an intrinsic limitation: successful reactivity typically requires substrates capable of engaging in productive complexation, usually dictated by specific electronic complementarity.[81,82] As a result, EDA-based borylations often rely on pre-functionalized substrates—such as Katritzky salts and sulfenyl-activated derivatives—whose electronic profiles are tailored to facilitate charge-transfer interactions.[84,86,87]

To circumvent these constraints and further broaden the scope of metal-free radical borylation, chemists have increasingly turned to an alternative activation mode: hydrogen atom transfer (HAT). Unlike EDA activation, HAT does not require pre-association between reagents. Instead, photoexcited HAT catalysts directly abstract a hydrogen atom from native C–H bonds, generating carbon radicals that can be intercepted by diboron reagents (Scheme 16).[88] This mechanistic shift greatly broadens the accessible substrate space, enabling radical borylation to proceed not only from pre-functionalized electrophiles but also from simple, abundant hydrocarbons. As a result, HAT-based activation offers a powerful new entry point to alkyl boronates directly from unactivated feedstocks.[64,65,88]

HAT-based radical borylation typically employs photoactive HAT catalysts, including benzophenone derivatives, polyoxometalates, diaryl ketones, and thiol or amine hydrogen-

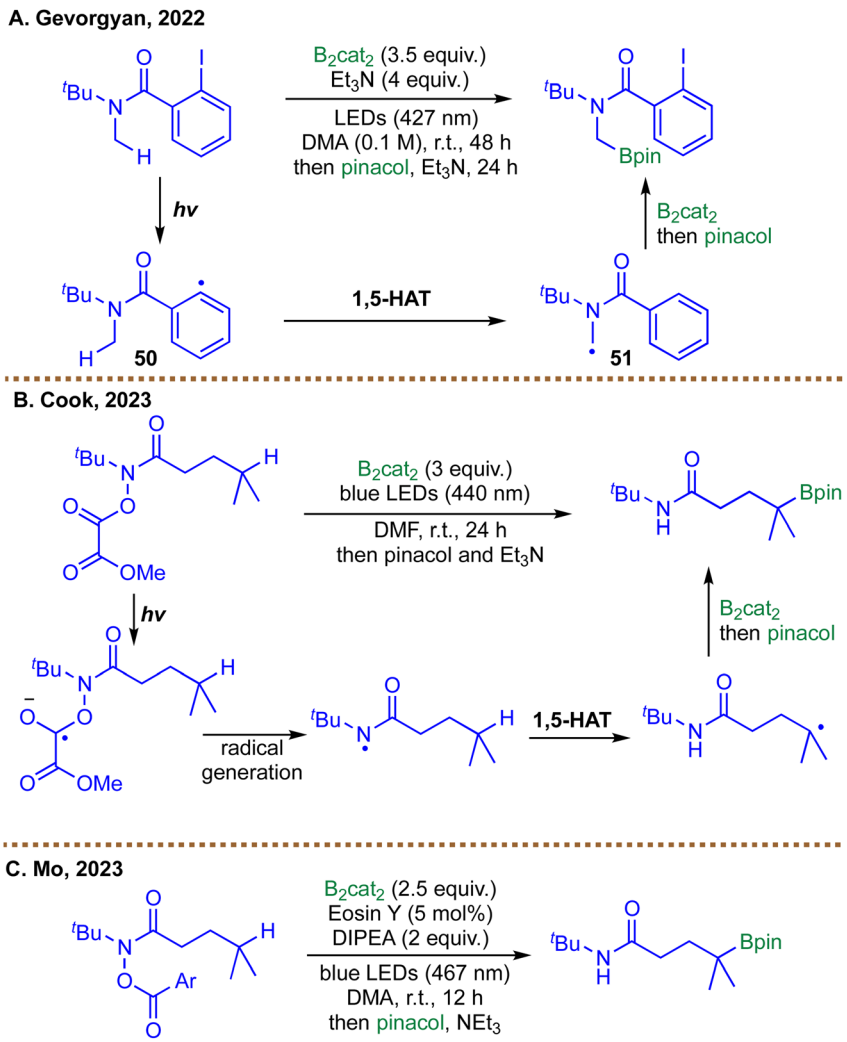

Scheme 18 Metal-free photoinduced 1,5-HAT-directed C–H borylations; (A) C–H borylations by Gevorgyan *et al.* in 2022; (B) C–H borylations by Cook *et al.* in 2023; (C) C–H borylations by Mo *et al.* in 2023.

abstracting systems, often in combination with Lewis bases or alkoxide additives that tune the reactivity of diboron reagents.[65,88,89] While offering unmatched feedstock diversity, HAT mechanisms bring their own challenges. Regioselectivity can be difficult to control when multiple C–H sites compete for abstraction, and both oxygen and moisture readily quench key radical intermediates.[64,65] Reaction efficiency is further shaped by polarity matching between the carbon-centered radical and the diboron reagent, which can favor or disfavor productive trapping.[65,90] Beyond these practical considerations, important mechanistic questions remain unresolved, particularly regarding the relative contributions of energy transfer, electron transfer, and subsequent radical coupling steps.[63,64]

In 2020, Noble and Aggarwal disclosed a metal-free strategy for photoinduced borylation of unactivated C(sp^3)–H bonds in simple alkanes, enabled by a chlorine-radical HAT manifold operating under remarkably mild conditions.[65] Diverging from conventional transition-metal-catalyzed borylations, which are typically restricted to aromatic and benzylic C–H bonds, the method employs a Cl˙-mediated HAT process initiated by violet-light photoexcitation of an *N*-alkoxyphthalimide oxidant **39**. Upon irradiation, **39*** is reductively quenched by B_2cat_2 to generate radical anion **40**, which undergoes β-scission to furnish trifluoroethoxy radical **48**. Oxygen-centered radicals are known to react with catechol boronic esters to form radical 'ate' complexes; the authors propose that **48** reacts with ClBcat through such an intermediate **41**, ultimately releasing a chlorine radical capable of HAT. Abstraction of a hydrogen atom from the alkane by either free Cl˙ or complex **41** produces HCl, alkyl radical **43**, and trifluoroethyl borate **42**. The alkyl radical **43** is then trapped by B_2cat_2, likely *via* a chloride-assisted radical complex **46** that facilitates B–B bond cleavage to furnish corresponding boronic esters. Finally, SET from the chloride-stabilized boryl radical **49** to the oxidant **39** regenerates the chlorine-transfer species **41**, closing the catalytic cycle. A particularly noteworthy aspect of this system is the unconventional HAT selectivity of the chlorine radical–boron 'ate' complex **41**, which displays a pronounced preference for stronger methyl C–H bonds over weaker secondary, tertiary, or benzylic positions. This inversion of classical radical reactivity underscores the unique electronic environment imparted by the boron–chlorine 'ate' structure. Although current limitations in yield and substrate stoichiometry warrant further refinement, this radical-mediated C–H borylation mode uniquely enables the conversion of simple hydrocarbon feedstocks into organoboron products with selectivity patterns distinct from those of traditional methodologies (Scheme 17).

Building on the concept of using tailored HAT reagents to unlock unconventional site selectivity, subsequent developments have explored alternative strategies for generating carbon-centered radicals poised for borylation. In Noble and Aggarwal's system, the key HAT agent is the chlorine radical–boron 'ate' complex **41**, which selectively abstracts hydrogen from stronger, less sterically encumbered methyl C–H bonds before the resulting alkyl radical is intercepted by B_2cat_2.[65] In contrast, the methods reported by Gevorgyan,[91] Cook,[92] and Mo[93] achieved positional control through intramolecular 1,5-HAT of amidyl radicals. Gevorgyan's method utilizes an easily installed 2-iodobenzoyl directing group: photoinduced C–I bond homolysis generates an aryl radical **50**, which undergoes a polarity-matched 1,5-HAT to furnish a nucleophilic α-aminoalkyl radical **51**, subsequently captured by B_2cat_2 to give the corresponding boronic esters (Scheme 18A).[91] The Mo and Cook protocols instead rely on hydroxamic acid derivatives (*O*-

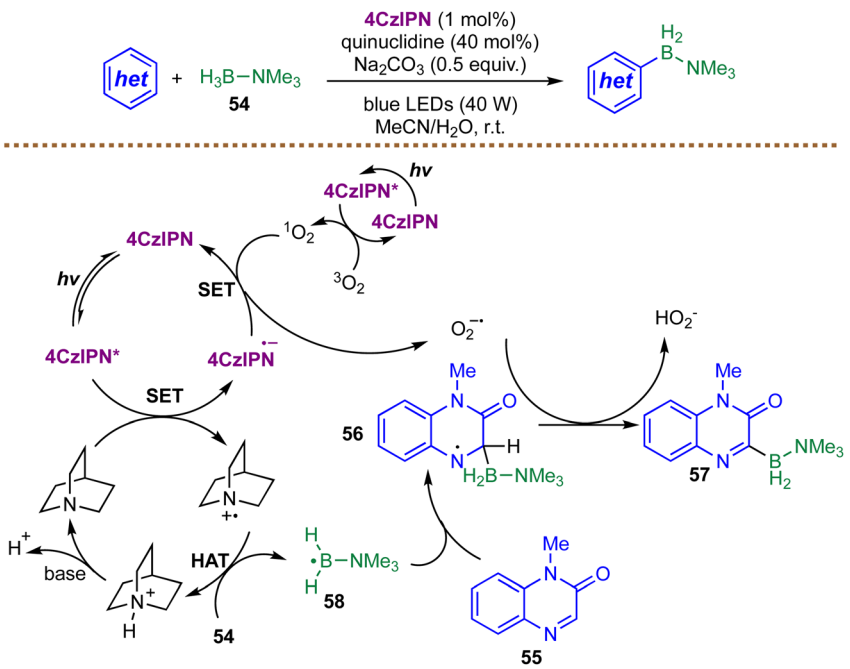

Scheme 19 C–H borylation of heterocycles by Liu *et al.*

benzoyl or *O*-oxalate) as precursors to amidyl radicals. These species are activated *via* photoreduction, either by an organic photocatalyst like Eosin Y or through direct excitation of a diboron-solvent adduct, initiating N–O bond cleavage to form an electrophilic amidyl radical. This radical then undergoes a 1,5-HAT to furnish a γ-carbon radical that is efficiently borylated by B_2cat_2 (Scheme 18B and C).[92,93]

Despite their distinct initiation pathways, these approaches ultimately converge on a shared chain-propagation manifold. In each case, the carbon-centered radical engages B_2cat_2 to form a transient borate complex, which undergoes homolytic B–B bond cleavage—often accelerated by Lewis-basic solvents or ancillary additives—to furnish the alkyl boronic ester.[91–93] This step simultaneously regenerates a boryl radical capable of sustaining the chain process.

Further expanding the repertoire of radical-mediated C–H borylation strategies, Liu and co-workers recently introduced a metal-free protocol that merges photoredox and HAT catalysis for the direct borylation of heterocycles (Scheme 19).[94] In this system, visible-light excitation of 4CzIPN generates the oxidized photocatalyst, which converts quinuclidine into a quinuclidinium radical cation. Hydrogen abstraction from Me_3N–BH_3 **54** by this quinuclidinium radical cation generates the key boryl radical intermediate **58**. This species adds regioselectively to electron-deficient heterocycle **55**, forming aminyl radical intermediate **56**. Concurrently, the reduced photocatalyst reduces singlet oxygen to superoxide ($O_2^{\bullet-}$), which mediates a two-step oxidative sequence: initial oxidation of radical intermediate **56** followed by deprotonation provides the borylated product **57**. The proposed radical pathway is supported by several mechanistic experiments. Radical-trapping reagents such as TEMPO or 1,1-diphenylethylene markedly suppress product formation, and the presence of a boryl radical intermediate is further corroborated by its interception with a trifluoromethylalkene to afford a defluoroborylation product. Moreover, singlet-oxygen quenching studies implicate the participation of $O_2^{\bullet-}$ in the oxidative step. The reliance on air as a terminal oxidant and the operational simplicity of the dual-catalytic platform afford broad functional-group tolerance and enable late-stage modification of complex pharmaceutical scaffolds under mild conditions. Nevertheless, because the mechanism relies on boryl radical addition to electron-deficient heterocycles, the method may not translate well to electron-rich heterocycles or non-heterocyclic substrates.

3.1.4 Photoinduced radical borylations *via* energy transfer (EnT). In contrast to photoredox catalysis, EnT catalysis operates through photosensitizers that absorb (visible) light and transfer their excited-state energy to a substrate without engaging in electron transfer.[95,96] Because no redox event is required, EnT activation circumvents the need for matched redox potentials and instead depends on favorable triplet–triplet energy transfer: the sensitizer must possess a higher triplet energy than the substrate, enabling exergonic energy migration.[95]

EnT-based radical borylation is particularly well-suited to substrates with accessible triplet states, such as aryl halides, heteroarenes, and certain strained or electron-deficient

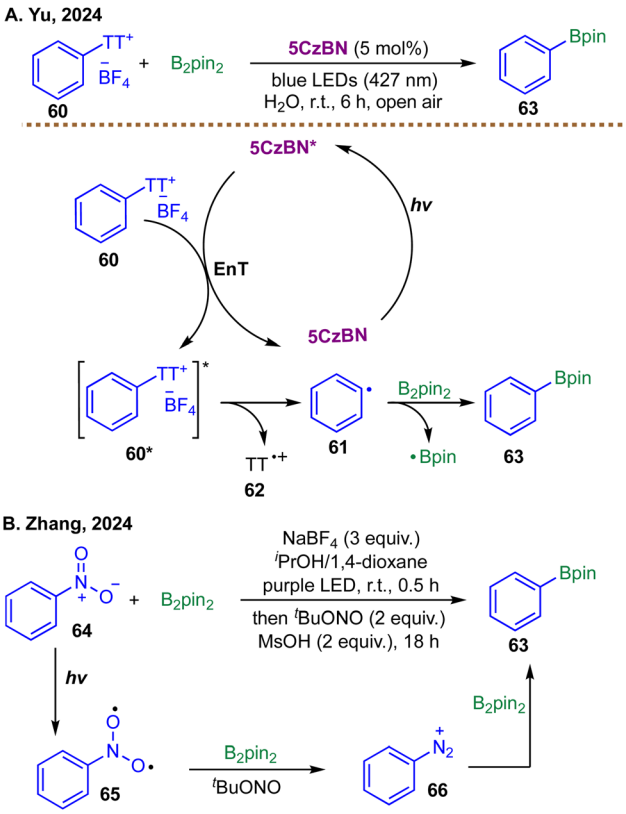

Scheme 20 EnT-enabled photocatalytic borylations; (A) borylation of thianthrenium salts by Yu *et al.* in 2024; (B) denitrogenative borylation of nitroarenes by Zhang *et al.* in 2024.

systems.[95,97,98] Key advantages include broad functional-group tolerance, reduced sensitivity to redox-active motifs, and the ability to activate substrates that are difficult to engage under SET conditions.[97–99] However, EnT catalysis also presents characteristic limitations. Suitable substrates must satisfy stringent triplet-energy requirements, which narrows the accessible chemical space, and the intrinsic sensitivity of triplet states to molecular oxygen necessitates strictly inert conditions.[100,101] In many cases, EnT pathways also provide less tunable chemo- or regioselectivity than redox-controlled or polarity-matched mechanisms.[95,102] Several mechanistic questions remain unresolved, including the precise identity of the reactive species generated upon triplet sensitization and the extent to which energy-transfer manifolds compete with unintended SET processes.[95]

A representative illustration of these concepts comes from the recent work of Yu and co-workers. In 2024, they reported a metal-free, EnT-driven strategy for the generation of aryl radicals from thianthrenium salts (Scheme 20A).[97] Unlike previous methods that relied on SET from a photocatalyst or within an EDA complex—both requiring stoichiometric electron donors—this process harnesses the excited triplet state of the organic photocatalyst 2,3,4,5,6-penta(carbazol-9-yl) benzonitrile (5CzBN). Mechanistic studies, including Stern–Volmer quenching, transient absorption spectroscopy, and catalyst evaluation, confirmed that the key activation step

involves triplet–triplet EnT from 5CzBN* to the aryl thianthrenium salt **60**. Excitation populates the triplet state of the salt **60**, which subsequently undergoes homolytic cleavage of the C–S bond to liberate the desired aryl radical **61** and a thianthrene radical cation **62**. The resulting aryl radical **61** is then efficiently trapped by B_2pin_2 to furnish the corresponding aryl boronic ester **63** in excellent yield. The authors report only a single example of radical borylation, leaving the generality of this transformation largely unexplored. Beyond borylation, this versatile EnT platform also enables deuteration, cyanation, arylation, and selenylation, and, crucially, it operates without the need for external sacrificial reductants, representing a notable advance in the metal-free generation and functionalization of aryl radicals.

Building on the theme of metal-free, EnT-enabled aryl radical generation, alternative strategies have emerged that leverage direct substrate excitation to access reactive intermediates for borylation. In the same year, Zhang and co-workers reported a visible-light-induced cascade denitrogenative process for the one-pot conversion of nitroarenes to arylboronates (Scheme 20B).[98] The proposed mechanism begins with photoexcitation of the nitroarene substrate **64** under purple LED irradiation, generating a triplet nitrene-like species **65** *via* the $n \rightarrow \pi^*$ transition. This excited-state intermediate **65** is subsequently reduced by B_2pin_2, which serves both as a reductant and a boryl source, forming an aryl diazonium intermediate **66**. The diazonium species is then trapped by B_2pin_2 to afford the corresponding aryl boronic ester **63**, completing the transformation under mild, metal-free conditions.

While both approaches achieve metal-free aryl radical borylation under visible-light irradiation, Yu and co-workers relied on a dedicated organic photocatalyst to mediate triplet–triplet energy transfer,[97] whereas Zhang and co-workers exploited direct photoexcitation of the nitroarene substrate itself,[98] highlighting an alternative strategy that bypasses an external photocatalyst.

3.1.5 Miscellaneous photoinduced radical borylations. Beyond the well-defined categories of SET-, EDA-, HAT- and EnT-mediated radical borylations, a variety of emerging strategies have been reported that do not neatly fit into these conventional activation modes. In 2020, Gong *et al.* reported a visible-light-induced borylation of unactivated tertiary alkyl methyl oxalates (Scheme 21).[103] Key to their mechanism is the formation of a $(DMF)_2$–B_2cat_2 adduct **70**, which weakly absorbs light at 450 nm to generate a boryl radical **71**. This radical adds to the carbonyl oxygen of oxalate **67**, forming intermediate **68** and triggering C–O bond cleavage and decarboxylation to yield a tertiary alkyl radical **69**. Subsequent homolytic substitution occurs at the B–B bond of B_2cat_2, yielding the corresponding alkyl boronic ester and regenerating the boryl radical **71**, thereby sustaining a radical chain process. The method performs well for tertiary alkyl methyl oxalates but shows no reactivity toward secondary alkyl oxalates and only moderate reactivity with the imidazole-modified L-carbothioate, which enables conversion of secondary alcohols to the corresponding boronates. Notably, the developed conditions are ineffective for primary substrates.

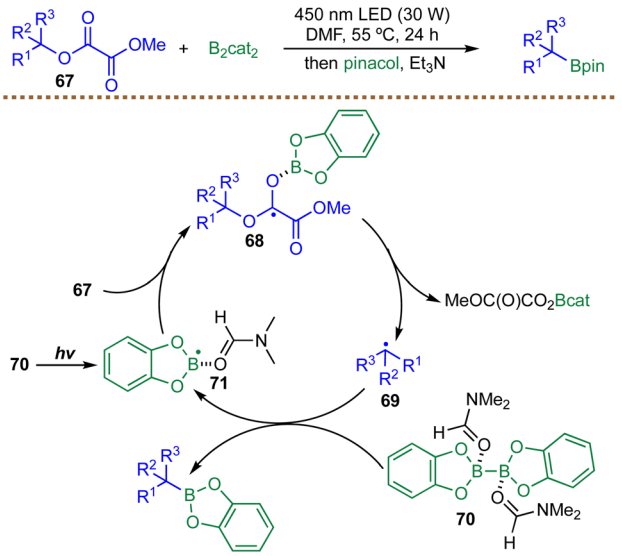

Scheme 21 Photoinduced alkyl C–O bond borylation.

Recent advances in metal-free radical borylation have unveiled a variety of innovative strategies for activating aryl halides and polyfluoroarenes under mild conditions. In one notable example, Chen *et al.* developed a visible-light-induced thiolate-catalyzed defluoroborylation of polyfluoroarenes using NHC–boranes (Scheme 22A).[104] The transformation proceeds *via* initial formation of a boryl sulfide intermediate, which undergoes homolytic cleavage under irradiation to generate NHC-boryl and thiyl radicals. The boryl radical adds regioselectively to the polyfluoroarene, and the resulting radical intermediate is subsequently reduced by a photoexcited aryl thiolate, promoting fluoride expulsion and formation of the borylated product. Notably, this strategy requires no external photocatalysts and showcases the dual role of thiolates as both catalysts and light-absorbing species. Although the method performs well with electron-deficient arenes, electron-rich aromatic systems are largely unreactive under the defluoroborylation conditions. Moreover, because the strategy fundamentally depends on radical C–F activation, substrates lacking suitably activated C–F bonds fall outside its effective scope.

In a complementary study, Ma and co-workers reported a transition-metal-free aqueous-phase borylation of aryl halides catalyzed by 1-methylbenzimidazole (Scheme 22B).[105] In this system, water facilitates the activation of B_2pin_2 *via* hydroxide addition to generate a nucleophilic boron complex **73**. Under UV irradiation, this complex undergoes homolytic B–B bond cleavage to generate boryl radical **75** and imidazole-boron radical **74**. The boryl radical anion **75** then reduces the aryl halide to form an aryl radical **76**, which couples with radical **74** to furnish the corresponding arylboronic ester. This methodology is entirely free of transition metals and organic solvents, relying on water as both solvent and the activator. Together, these methodologies highlight the expanding potential of photochemical and radical-based strategies in metal-free borylation, further enriching the growing toolkit available for radical borylation transformations.

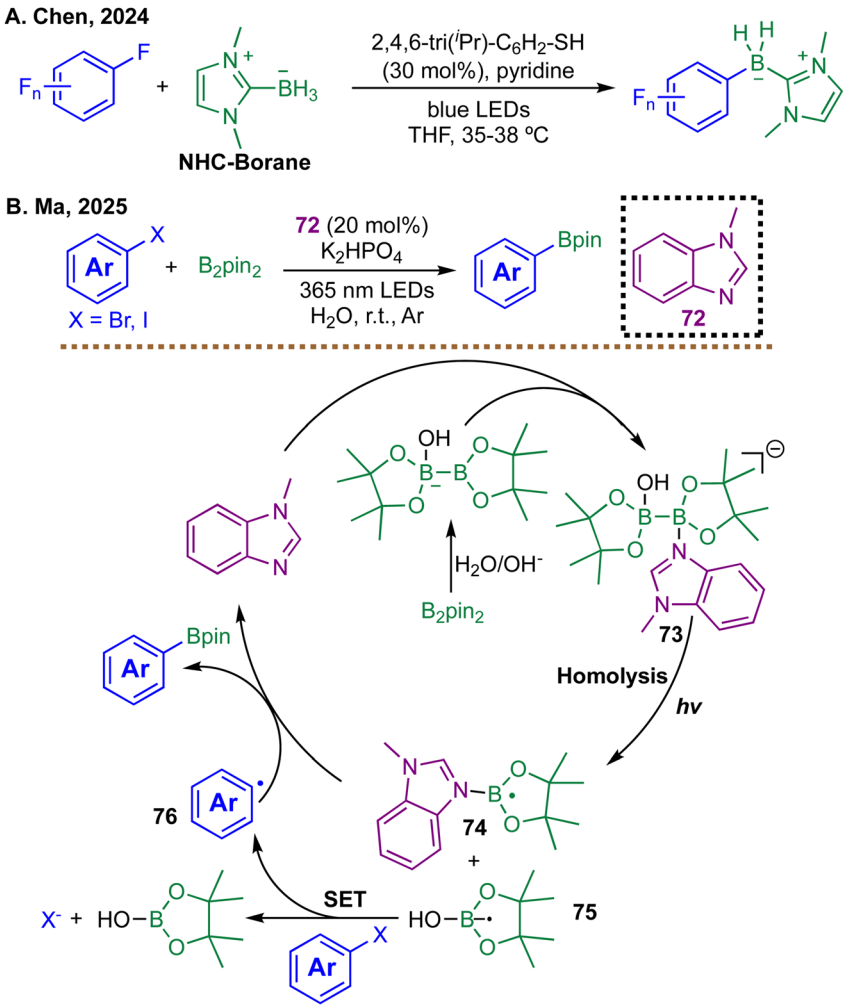

Scheme 22 Photoinduced borylations *via* boryl radicals; (A) borylation of polyfluoroarenes by Chen *et al.* in 2024; (B) borylation of aryl halides by Ma *et al.* in 2025.

3.2 Radical borylations *via* electrochemistry

In recent years, electrochemical methods have emerged as powerful tools for metal-free radical borylation, providing attractive alternatives to traditional transition-metal or photoredox catalysis. By using electricity as the driving force for single-electron transfer, electrochemical approaches allow precise control over redox potentials, enabling the generation of carbon-centered radicals under mild conditions.[106] These strategies have been successfully applied to a broad array of substrates, including aryl halides, redox-active esters, ammonium salts, alkyl alcohol derivatives, and even unactivated C–H bonds, thereby expanding the accessible chemical space for radical borylation.[34,106–111] Typical reaction platforms employ borylating reagents such as B_2pin_2, B_2cat_2, or HBpin, often in combination with bases or Lewis bases (*e.g.*, alkoxides, carbonates, and amines) that modulate the nucleophilicity or activation mode of the borylating species.[112,113] This electrochemical control not only enables catalyst-free conditions but also minimizes the need for high-energy light sources or sacrificial reagents.

Despite these advantages, electrochemical radical borylation faces characteristic constraints that shape substrate scope and mechanistic design. Reactions are intrinsically governed by redox compatibility, as substrates must possess reduction potentials accessible within the electrochemical window of the solvent–electrolyte system.[113,114] Highly electron-rich or strongly electron-deficient substrates can therefore fall outside the operational range unless paired with mediators or redox shuttles. Sensitivity to oxygen and moisture remains a practical limitation, as radical intermediates and activated diboron species are readily quenched under aerobic conditions.[115] Unresolved mechanistic questions persist regarding the interplay between direct and mediated electron transfer, the nature of key boryl radical or boryl anion species at the electrode surface, and the degree to which the electrode material participates in radical propagation.[116,117] Continued advances in *operando* spectroscopy and electroanalytical techniques are expected to clarify these issues, further unlocking the potential of electrochemistry in radical borylation chemistry.

Building on the growing utility of electrochemical strategies for radical borylation, Xu *et al.* reported in 2021 an electrochemically promoted decarboxylative borylation of alkyl N, *N*-hydroxyphthalimide (NHP) esters using B_2cat_2 in an undivided cell (Scheme 23A).[108] In this system, cathodic reduction of the NHP esters generates a radical anion that undergoes rapid decarboxylation to furnish an alkyl radical. This radical then reacts with B_2cat_2 in the presence of DMF to form a boron-centered intermediate, which ultimately delivers the corresponding alkyl boronic ester after transesterification with pinacol. Mechanistic studies, including radical trapping and radical-clock experiments, support a chain-propagation pathway initiated by electrochemical reduction. This work demonstrates proof-of-concept electrochemical decarboxylative borylation from NHP esters, highlighting the feasibility of metal-free electro-initiation, but it is limited in depth of mechanistic and scale-up data.

Using similar redox-active esters (RAEs) as radical precursors, Baran *et al.* developed an electrochemical decarboxylative borylation protocol using inexpensive carbon electrodes and LiBr as an electrolyte (Scheme 23B).[109] Mechanistic studies, including cyclic voltammetry and kinetic analysis, revealed that B_2cat_2 and the RAE form a precomplex **79** that undergoes single-electron reduction at the cathode. This rate-limiting reduction triggers decarboxylation to generate an alkyl radical **81**, which subsequently reacts with a DMF–B_2cat_2 adduct **78** to afford the

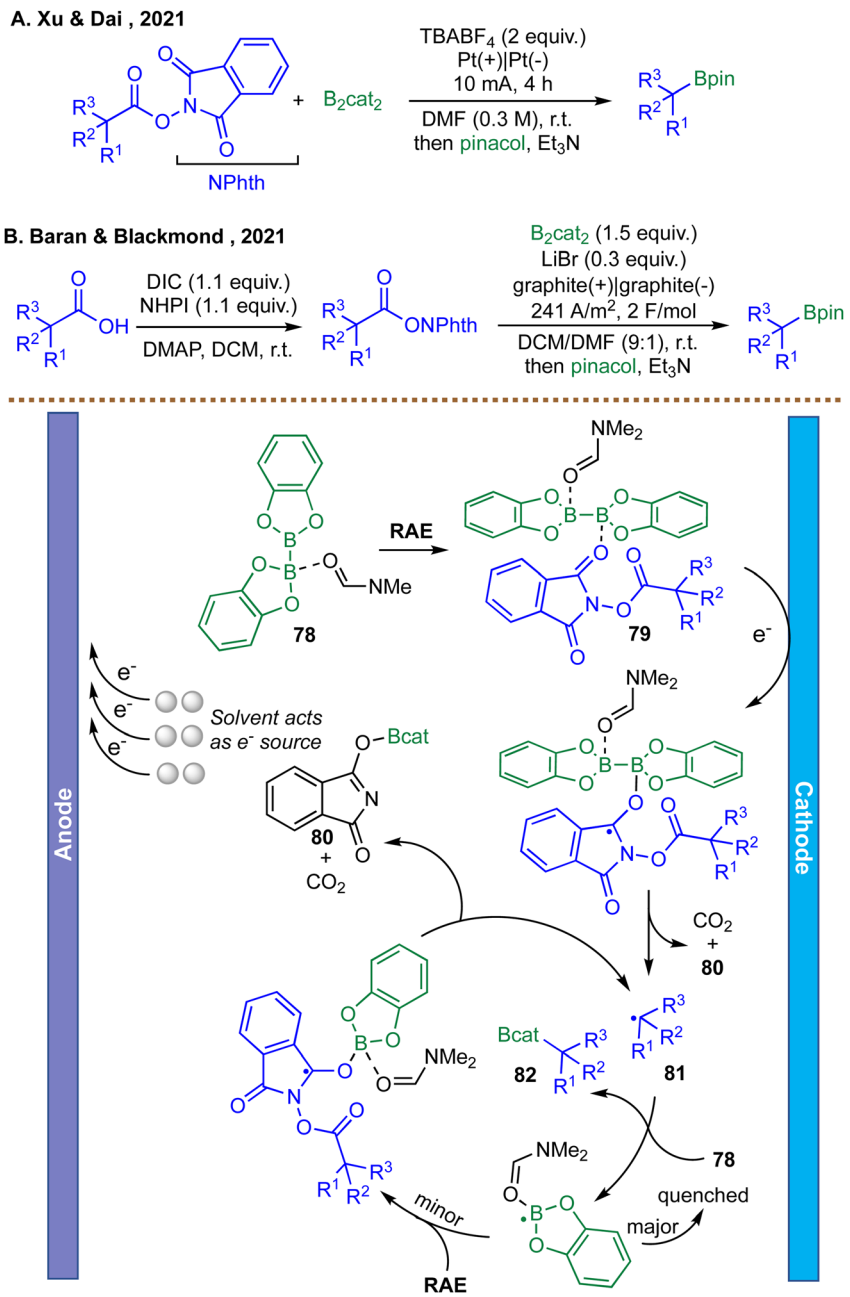

Scheme 23 Electrochemical borylation of carboxylic acids and their derivatives; (A) decarboxylative borylations by Xu and Dai *et al.* in 2021; (B) decarboxylative borylations by Baran and Blackmond *et al.* in 2021.

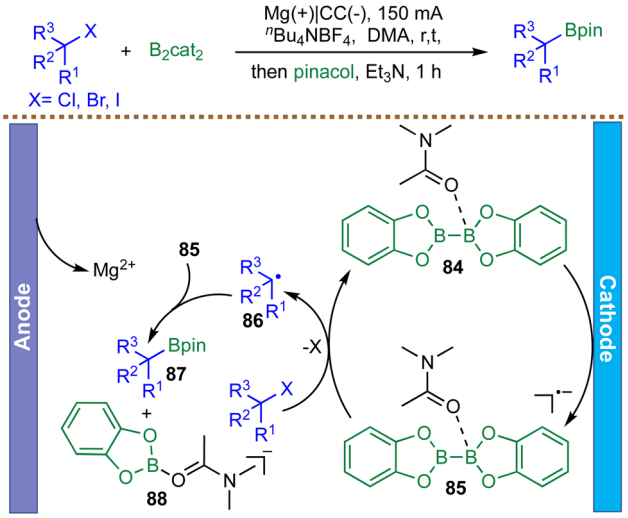

Scheme 24 Electrochemical borylation of alkyl halides.

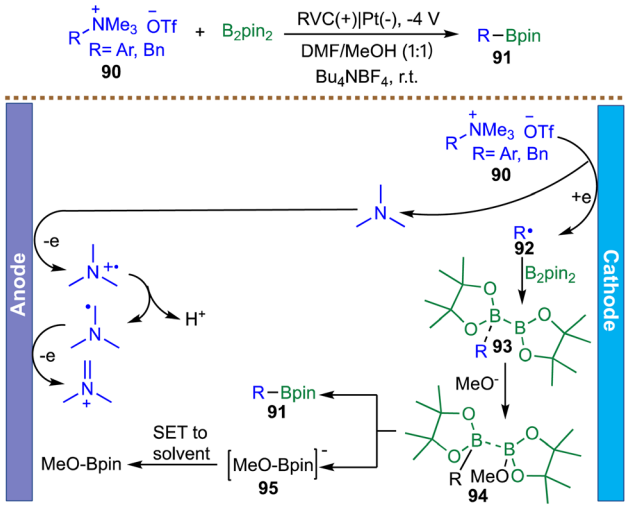

Scheme 25 Electrochemical borylation of aryl and benzyl ammonium salts.

borylated product **82**. The reaction exhibits zero-order kinetics in both substrates, indicating a mechanism dominated by electrochemical initiation rather than radical chain propagation. This method exhibits broad substrate scope, including primary, secondary, and tertiary substrates and natural products and drug derivatives. The transformation has been successfully scaled up in batch to 40 mmol, affording the corresponding boronic ester in 40% yield, comparable to the 35% yield obtained on a 0.1 mmol scale. Furthermore, a 100 g scale reaction was performed in a flow system ($LiBF_4$, 0.2 M; 1.8 A; 2.5 F mol^{-1}; 1500 mL min^{-1}), delivering the corresponding boronic ester in 60% yield, consistent with small batch results.[109] While the study provides a detailed and experimentally grounded mechanistic understanding, the substrate scope remains predominantly limited to alkyl substrates, with (hetero)aryl substrates yet to be thoroughly examined.

Moving beyond NHP esters, which require prior synthesis from carboxylic acids, Wang *et al.* reported in 2021 an electrochemical, metal-free borylation of readily available unactivated alkyl halides (X = I, Br, Cl) using B_2cat_2 as both the boron source and a redox mediator (Scheme 24).[110] The reaction proceeds under constant current electrolysis at room temperature and exhibits broad functional group tolerance, accommodating primary, secondary, and tertiary alkyl halides, including derivatives of natural products and pharmaceuticals. Mechanistic investigations, including cyclic voltammetry, radical clock experiments, and DFT calculations, support a radical-based pathway. DMA coordinates to B_2cat_2 to form complex **84**, which undergoes cathodic reduction to generate intermediate **85**. This intermediate mediates the reduction of alkyl halides *via* a highly exergonic electron transfer, generating alkyl radicals **86**. These radicals then undergo barrier-less radical–radical cross-coupling with the persistent boryl radical species **85** to form alkyl boronates **87**. By circumventing the high reduction potentials of alkyl halides, especially chlorides and bromides, this mediator strategy enables efficient borylation without the need for transition-metal catalysts or photoredox activators.

Extending electrochemical radical borylation beyond halide substrates, Xu and co-workers developed a complementary metal-free protocol for the borylation of aryl- and benzyltrimethylammonium salts using B_2pin_2 (Scheme 25).[111] This strategy leverages the inherent electroreductivity of quaternary ammonium groups, which undergo direct cathodic single-electron reduction to furnish aryl and benzyl radicals **92** without the assistance of a redox mediator. The mechanism is proposed to begin with reductive cleavage of the C–N bond in ammonium salt **90**, generating a carbon-centered radical **92** that is subsequently trapped by B_2pin_2in in the presence of methoxide. This sequence proceeds through intermediates **93** and **94** to deliver the desired borylated product **91** along with anion **95**. Concurrent anodic oxidation of the solvent balances the overall redox process, and the resulting anion **95** ultimately undergoes single-electron quenching to form MeO-Bpin. Mechanistic support for a radical pathway is provided by

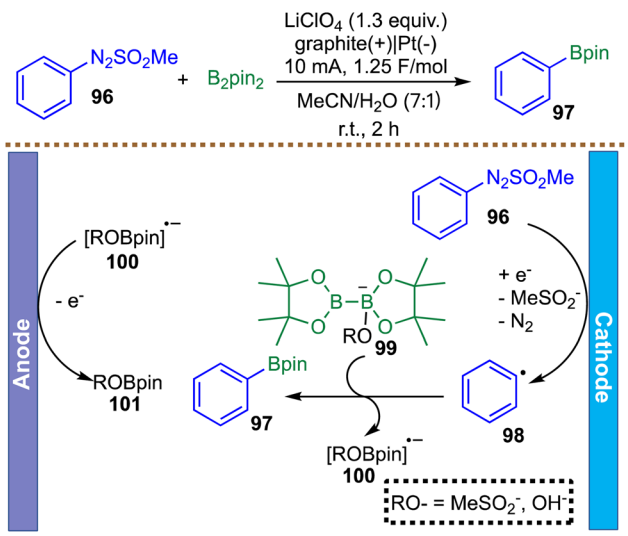

Scheme 26 Electrochemical borylation of arylazo sulfones.

complete inhibition of product formation in the presence of TEMPO. Notably, this C–N activation platform exhibits excellent functional group tolerance, particularly towards halides (Cl and Br), which are typically problematic in transition-metal-catalyzed borylation protocols due to competitive oxidative addition. Although the reported scope includes a range of aryl and benzyl ammonium salts, the method has not been demonstrated for simple, unactivated alkyl ammonium substrates. Consequently, its applicability is largely confined to aryl and benzylic radical generation rather than representing a broadly general C(sp^3) borylation platform.

Beyond electroreductive activation of C–N and C–X bonds, electrochemical strategies have also been extended to alternative radical precursors that enable complementary reactivity. In this context, Yi *et al.* reported a metal-free electrochemical borylation of arylazo sulfones, distinguished by a paired electrolysis design that simultaneously engages both anodic and cathodic processes (Scheme 26).[118] This method enables the efficient synthesis of aryl boronates from B_2pin_2 with broad functional group tolerance, and its practicality is highlighted by a gram-scale demonstration that delivers the product in 73% isolated yield. Mechanistically, the transformation parallels the C–S bond-forming process described in their work. The catalytic cycle is initiated by single-electron reduction of the arylazo sulfone **96** at the cathode, generating a phenyl radical **98**. This radical is then intercepted by a base-activated diboron species **99** to form the C–B bond, delivering the product **97** and a radical anion byproduct **100**. Anodic oxidation of this radical anion **100** then regenerates the active boron species **101**, completing the cycle and maintaining overall redox neutrality. The study serves primarily as a proof-of-concept for the radical borylation of arylazo sulfones, having explored only a limited set of aryl substrates. Consequently, its applicability to aliphatic systems remains untested, and the broader generality of the method in radical borylation is uncertain.

In addition to arylazo sulfones, electrochemistry provides a platform to leverage arylhydrazines—readily accessible and stable building blocks—as efficient precursors for aryl radical generation. In 2022, Zhang and co-workers reported an electrochemical, metal-free strategy for the C–N borylation of arylhydrazine hydrochlorides with B_2pin_2 (Scheme 27).[119] The proposed mechanism begins at the anode, where the free arylhydrazine **104**, generated *in situ* by deprotonation, undergoes single-electron oxidation. This step, potentially facilitated by the iodide anion from the $^nBu_4NI$ electrolyte, triggers sequential deprotonation and loss of dinitrogen to form a key aryl radical **105**. This radical is then trapped by a base-activated diboron species **106**, affording the aryl boronic ester **103**. The mechanism is supported by radical trapping experiments with TEMPO, which significantly suppress product formation. The electrochemical cycle is closed by cathodic proton reduction, producing hydrogen gas and maintaining overall redox neutrality. The borylation of phenylhydrazine hydrochloride was successfully scaled up to 7 mmol under the standard conditions, affording the corresponding phenyl Bpin in 56% yield, comparable to the result obtained on a 0.3 mmol scale (58%).[119] This protocol thus represents a scalable, transition-metal-free approach for accessing aryl boronic esters from stable and readily available arylhydrazine precursors. Despite these advantages, the substrate scope has been largely limited to simple arylhydrazines, with little exploration of aliphatic or heteroaryl substrates.

Nitroarenes are abundant feedstock chemicals and common motifs in pharmaceuticals, yet their broad application has been limited by the scarcity of general methods for denitrative functionalization. In 2023, Zhang *et al.* reported an electrochemically mediated borylation of nitroarenes to furnish a wide range of aryl boronic esters at room temperature under mild conditions (Scheme 28).[120] This transformation demonstrates excellent functional-group tolerance, enabling the straightforward synthesis of aryl boronic esters bearing halogen, ester, nitrile, alkenyl, and (hetero)aryl substituents. Mechanistic

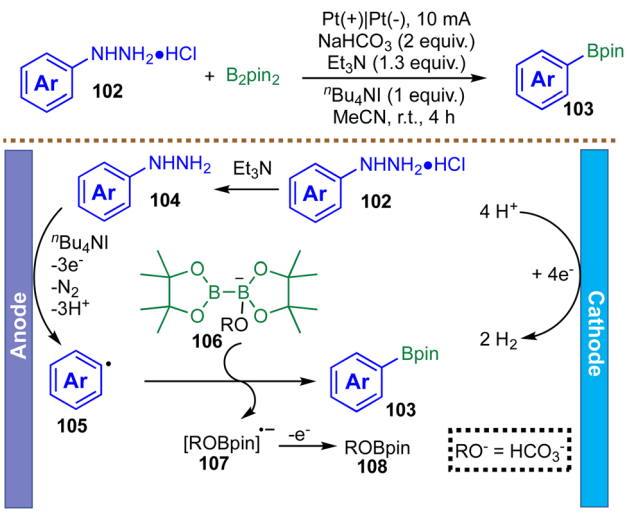

Scheme 27 Electrochemical C–N borylation of arylhydrazines.

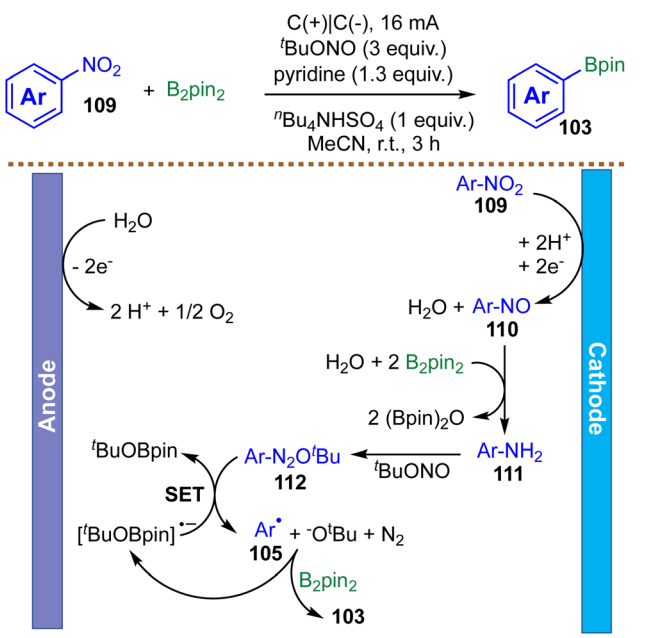

Scheme 28 Electrochemical borylation of nitroarenes.

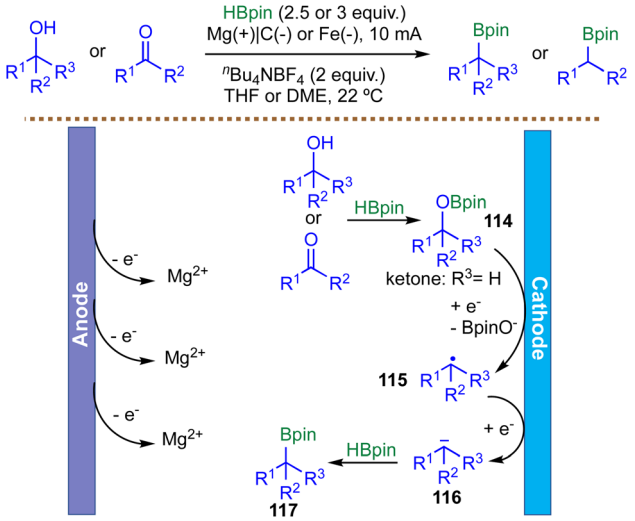

Scheme 29 Electrochemical borylation of alcohols and carbonyls.

investigations, including radical-trapping experiments and cyclic voltammetry, support a radical cascade initiated by electrochemical reduction. The proposed pathway begins with cathodic reduction of the nitroarene **109** to a nitroso intermediate **110**, which subsequently reacts with B_2pin_2 and water to generate an aniline **111** *in situ*. This aniline **111** then undergoes a classic Sandmeyer-type borylation: diazotization with *tert*-butyl nitrite (^{t}BuONO) forms a diazonium salt **112**, which undergoes single-electron fragmentation to liberate nitrogen gas and generate a key aryl radical **105**. This aryl radical **105** then reacts with B_2pin_2 to ultimately deliver the borylated product **103**.

Alcohols and carbonyl compounds are abundant in organic molecules, making the development of new strategies for their activation and functionalization highly valuable for the synthesis and derivatization of natural products and pharmaceuticals. In a significant advance for electrochemically driven borylation, Lin *et al.* developed a unified deoxygenative borylation strategy for alcohols, aldehydes, and ketones that operates *via* a unique radical-polar crossover mechanism (Scheme 29).[121] A key feature of this strategy is the dual role of pinacolborane: beyond serving as the boron source, HBpin acts as an *in situ* activator, converting the substrate into a redox-active trialkylborate intermediate **114**. This intermediate **114** possesses a significantly lowered reduction potential, enabling efficient cathodic reduction under mild electrochemical conditions. The transformation proceeds through an ECE (Electron transfer–Chemical reaction–Electron transfer) sequence. Initial reduction of intermediate **114** generates an alkyl radical **115**, which undergoes a second reduction to form a carbanion **116**. Trapping of this carbanion **116** by a second equivalent of HBpin furnishes the alkyl boronate **117**. This elegant polarity-inversion strategy effectively transforms native alcohol or carbonyl functionalities into carbanion equivalents, offering a mild, transition-metal-free route to alkyl boronic esters. Despite demonstrating efficient reactivity with benzylic and allylic systems, the authors did not investigate unactivated primary or secondary aliphatic alcohols. As a result, the generality of the protocol toward more challenging aliphatic substrates has yet to be established.

Aromatic chlorides are highly attractive feedstocks among aromatic halides due to their low cost and wide commercial availability. However, they remain the most challenging class to activate, owing to their very negative reduction potentials (<2 V *vs.* Fc/Fc$^+$) and strong C–Cl bond dissociation energies (>97 kcal mol^{-1}). In 2023, Milner *et al.* reported the first electroreductive radical borylation of unactivated (hetero)aryl chlorides, enabled by cumulene-based organic electrocatalysts, providing broad access to aryl boronic esters (Scheme 30).[113] Notably, this protocol efficiently engages electron-rich and electron-neutral aryl chlorides that were previously inaccessible under purely electrochemical conditions. Mechanistic investigations, including cyclic voltammetry, UV/Vis spectroscopy, and DFT

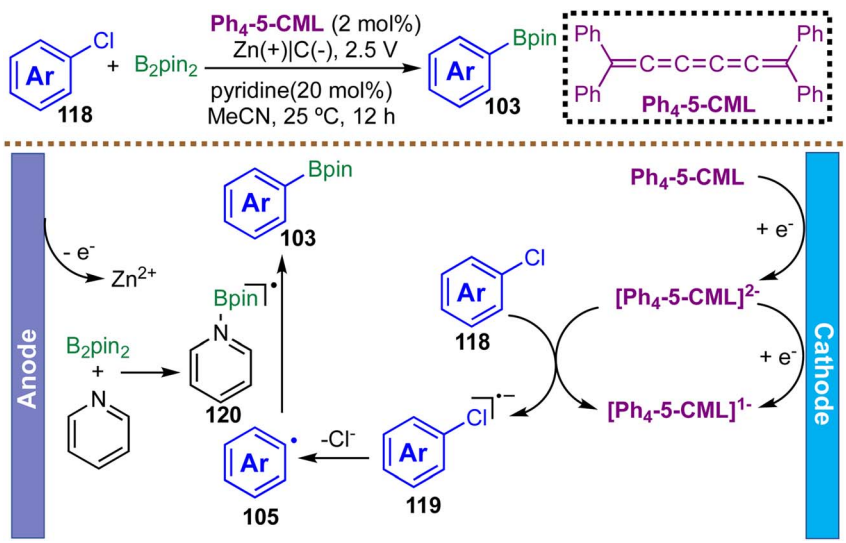

Scheme 30 Electroreductive radical borylation of unactivated (hetero)aryl chlorides.

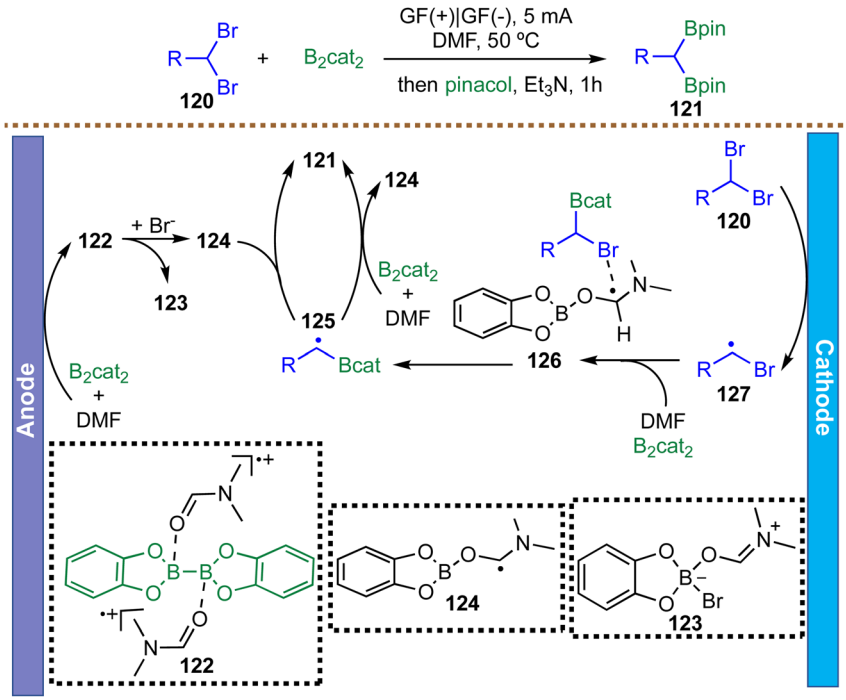

Scheme 31 Electrooxidative activation of B_2cat_2 to access *gem*-diborylalkanes.

calculations, support a stepwise electron transfer pathway. The doubly reduced cumulene (Ph_4–5-CML^{2-}) delivers a thermodynamically uphill SET to chloroarene, generating a radical anion intermediate. This species undergoes rapid, exergonic mesolytic C–Cl bond cleavage to afford an aryl radical and chloride ion. The aryl radical is subsequently trapped by B_2Pin_2 to form the corresponding boronic ester. Notably, the π-stacking interactions between the cumulene mediator and the arene substrate are proposed to lower the kinetic barrier for electron transfer, thereby enhancing catalytic efficiency. This work represents the first general electroreductive radical borylation of unactivated (hetero)aryl chlorides and exhibits broad compatibility with electron-rich, electron-neutral, and some heteroaryl substrates, providing efficient access to diverse aryl boronic esters. However, electron-poor chloroarenes, which possess lower-lying LUMOs, show diminished reactivity, likely due to less favorable SET energetics and weakened π-stacking interactions with the cumulene mediator.

Gem-diboronates are highly versatile synthetic intermediates, and in 2023, Lu *et al.* introduced the first electrochemical *gem*-diborylation of gem-bromides *via* a paired electrolysis strategy, enabling the efficient preparation of structurally diverse *gem*-diborylalkanes (Scheme 31).[122] The proposed mechanism is initiated by anodic single-electron oxidation of a DMF-ligated B_2cat_2 complex, generating a solvent-stabilized radical cation **122**. Both DFT calculations and cyclic voltammetry support a subsequent quasi-homolytic B–B bond cleavage, which proceeds with a low energy barrier to form a nucleophilic, DMF-coordinated boryl radical **124**. In parallel, the substrate **118** undergoes cathodic reduction to afford the corresponding carbon-centered radical **127**. The reaction of the intermediate **127** with B_2cat_2 and DMF produces the monoborylated radical **125** through intermediacy of **126**. Finally, a convergent radical–radical cross-coupling between radicals **124** and **125** delivers the *gem*-diborylated products **121**. This sequence provides a direct, mild, and redox-neutral route to *gem*-diborylalkanes without the need for external oxidants or reductants, highlighting the synthetic power of paired electrolysis in complex radical transformations.

While electrooxidative B–B bond activation provides a powerful route to *gem*-diborylalkanes, the development of

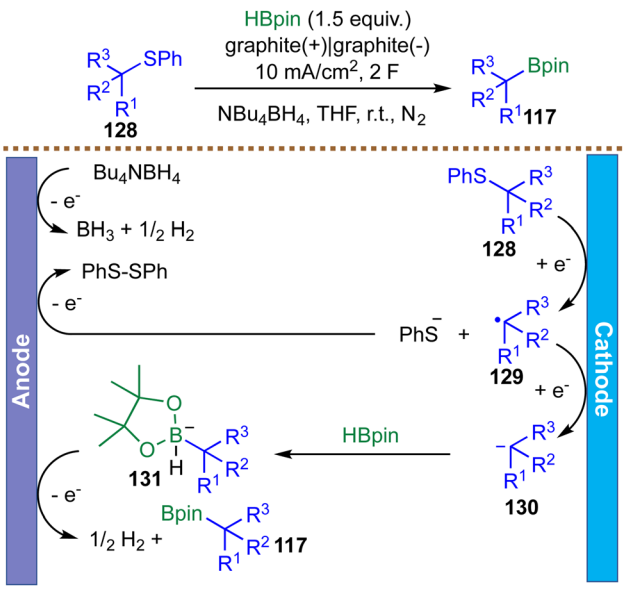

Scheme 32 Electrochemical desulfurative borylation of thioethers.

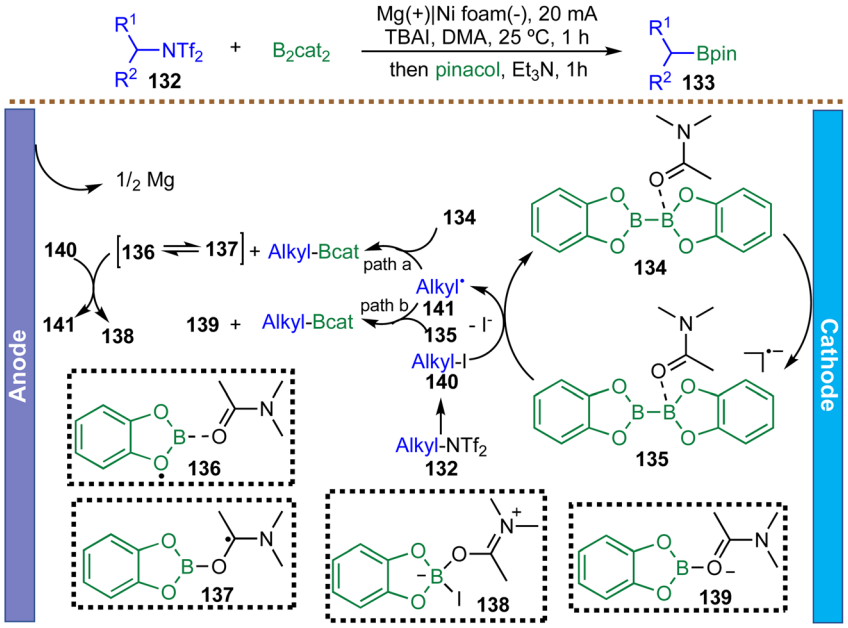

Scheme 33 Alkyl bistriflimidate-mediated electrochemical deaminative borylations.

complementary electroreductive strategies for converting abundant feedstock chemicals into boron-containing motifs is equally valuable. In 2024, Lundberg *et al.* reported an electrochemical desulfurative borylation of thioethers that proceeds through a distinct carbanionic pathway, contrasting sharply with conventional radical-based mechanisms (Scheme 32).[123] The proposed mechanism is initiated by cathodic single-electron reduction of the thioether substrate **128**, triggering mesolytic cleavage of the C(sp^3)–S bond to generate a phenylthiolate anion and a transient carbon-centered radical **129**. A critical radical-polar crossover occurs *via* a second SET, converting radical **129** into a stabilized carbanion **130**. This key intermediate **130** is then directly trapped by HBpin, which acts as an electrophile in this context, leading to the formation of the borohydride species **131**. Subsequent anodic oxidation of **131** releases the borylated product **117**. Charge balance within the paired electrolysis is maintained by oxidation of both the tetrabutylammonium borohydride (NBu_4BH_4) electrolyte and the phenylthiolate byproduct, producing H_2 and diphenyldisulfide, respectively. Compelling evidence for the carbanionic mechanism comes from a radical-clock experiment: a substrate capable of rapid 5-*exo*-trig cyclization furnished exclusively the linear borylation product, indicating the absence of a persistent free-radical intermediate. The method demonstrates good functional group tolerance and accommodates structurally complex pharmaceuticals and natural products. However, the substrate scope has been largely limited to allylic and benzylic systems, with other aryl and alkyl substrates remaining largely unexplored. A gram-scale reaction of benzyl(phenyl)sulfane produced benzyl Bpin in 77% yield (1 g, 6 mmol scale) under modified conditions (3 equiv. HBpin in MeCN), which is significantly lower than the 95% yield achieved on a 0.5 mmol scale.[123] This observation underscores a key limitation of electrochemical borylations: while they perform efficiently on a small scale, scaling up to preparative quantities remains challenging.

Aliphatic primary amines are ubiquitous in nature and in living organisms, serving as fundamental building blocks. In 2025, Wang *et al.* reported an electrochemical strategy utilizing alkyl bistriflimidates as novel radical precursors, generated *via* direct activation of primary alkyl amines with trifluoromethanesulfonic anhydride (Scheme 33).[124] This electrochemical protocol demonstrates broad functional group tolerance and has been successfully applied in continuous-flow setups, demonstrating scalability and practical applicability. Mechanistic studies, including intermediate trapping, cyclic voltammetry, and EPR spectroscopy, indicate a key halogen-atom transfer step: the iodide anion from the TBAI electrolyte rapidly converts the alkyl bistriflimidate **132** *in situ* into a more readily reducible alkyl iodide **140**. Cathodic reduction of **140** then generates the corresponding alkyl radical **141**. Borylation is proposed to proceed *via* one of the two pathways: either (a) direct addition of the alkyl radical **141** to a catecholborane-derived complex **134** or (b) a radical–radical cross-coupling between the alkyl radical **141** and the boronate radical anion **135**. Beyond borylation, the platform was extended to other deaminative functionalizations, including sulfuration, selenation, and sulfonylation, all proceeding *via* a similar radical pathway. Although the method exhibits broad applicability, yields for secondary and cyclic alkyl amines are only moderate, highlighting that the substrate structure can significantly impact reaction efficiency.

Taken together, recent advances in electrochemically assisted radical borylation provide a complementary and versatile toolkit for accessing both alkyl and (hetero)aryl boronic esters. These strategies harness diverse radical precursors—including halides, ammonium salts, thioethers, alcohols, carbonyl compounds,

amines, and nitroarenes—under mild conditions. Collectively, these developments highlight the growing potential of electrochemistry to enable efficient, selective, and practical C–B bond formation, expanding the synthetic repertoire for both complex molecule synthesis and late-stage functionalization.

3.3 Radical borylations *via* thermal activation

Radical borylation driven by thermal activation has emerged as a valuable complement to photochemical and electrochemical strategies. Its fundamental rationale lies in the ability of heat to induce homolysis or thermally driven single-electron transfer processes, enabling the generation of carbon-centered radicals from suitable precursors without the need for light or external redox inputs.[125,126] Many common functional groups, such as alkyl/aryl halides,[127] pyridinium salts,[128] peroxides,[125,129] diazonium salts,[126] and sulfonyl derivatives,[130] can undergo bond cleavage or reduction at elevated temperatures to release radicals. Once formed, these radicals can be efficiently trapped by activated diboron reagents, which serve as efficient radical acceptors when coordinated to bases or Lewis bases.[127,131]

Compared with photochemical or electrochemical approaches, thermally induced radical borylations circumvent the need for specialized irradiation equipment, photocatalysts, or electrolysis setups and often exhibit superior compatibility with strongly light-absorbing or photosensitive substrates. However, the elevated temperatures and reliance on relatively harsh radical initiators can restrict substrate scope and limit operational practicality. Mechanistic ambiguities also persist, including the precise identity and reactivity of the boryl radical or boryl anion species, the role of base–diboron adducts in radical generation, and the balance between chain propagation *versus* stepwise radical capture pathways.[63,131,132] Despite these challenges, thermal activation continues to provide a complementary and mechanistically rich platform for radical borylation, and ongoing advances continue to broaden both substrate scope and mechanistic understanding.

Building on the growing repertoire of thermally induced radical borylation strategies, Cornella *et al.* reported in 2020 an efficient deaminative radical borylation of aryl amines enabled by a tailored pyrylium reagent (Scheme 34).[128] This protocol provides efficient access to aryl boronic esters, exhibits broad functional group tolerance (*e.g.* halides, methoxy, amines, amides, carbonyls, and esters), and is readily scalable (84% yield, 1.23 g). The transformation begins with condensation of the primary amine with a sterically constrained pyrylium salt ^{sc}Pyry-OTf to form a non-planar, highly strained pyridinium intermediate **142**. This structural distortion destabilizes the C–N bond and furnishes the thermodynamic driving force for subsequent radical formation. A Lewis-base/diboron complex **146** then mediates SET reduction of the pyridinium species **142**, triggering homolytic C–N bond cleavage to generate the aryl radical **144**. This aryl radical **144** is rapidly trapped by B_2cat_2 to forge a new C–B bond. The use of a sterically hindered amide solvent $^{i}Pr_2NC(O)Me$ is crucial for suppressing undesired hydrogen atom transfer pathways that would otherwise generate reduced by-products. Mechanistic investigations, including EPR spectroscopy and radical trapping, support a radical chain process in which the solvent-ligated boron radical species **146** acts as the chain carrier, regenerating reactive intermediates and sustaining turnover. While this method provides a valuable route for transforming widely available aryl amines into aryl boronic esters, its overall step-economy is diminished by the required pre-activation through condensation with the pyrylium reagent. In addition, reliance on the costly, sterically hindered amide solvent $^{i}Pr_2NC(O)Me$ further increases the operational expense of the borylation process.

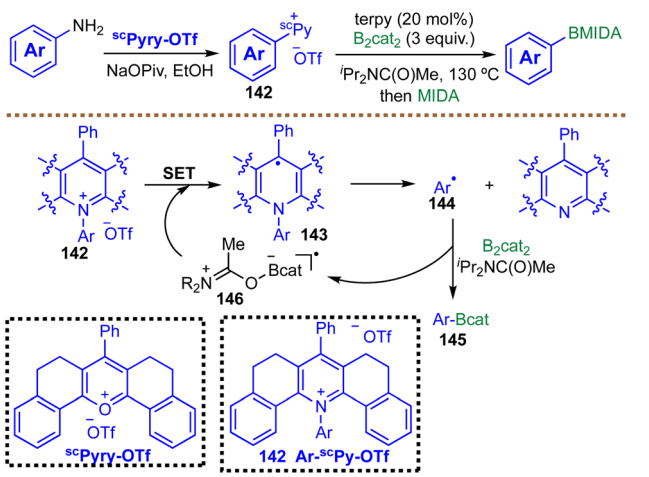

Scheme 34 Radical C–N borylation of aromatic amines enabled by a pyrylium reagent.

Sulfone functionalities are important and fundamental structural motifs in organic synthesis, making new strategies for their functionalization particularly valuable. In 2021, Marder *et al.* disclosed a base-mediated, metal-free radical borylation of alkyl sulfones using B_2neop_2, providing a direct and operationally simple route to alkyl boronic esters without the need for the transesterification steps commonly required when using B_2cat_2 (Scheme 35).[130] The reaction is proposed to initiate with the formation of an ate complex **149** from the alkyl sulfone **147**, B_2neop_2, and NaO^tBu. This intermediate **149** undergoes intramolecular SET to generate a boryl-containing radical **150** alongside a sulfone radical anion **151**. Fragmentation of **151** releases a phenylsulfinate anion and generates the alkyl radical **152**, which subsequently couples with radical **150** to afford the alkyl boronic esters **148** together with ^{t}BuOBneop. The radical nature of the transformation is unequivocally supported by multiple lines of evidence: radical clock substrates delivered cyclization products; radical scavengers such as TEMPO and BHT suppressed product formation and produced characteristic adducts; and EPR spectroscopy directly detected reactive radical intermediates. This work establishes alkyl sulfones as efficient radical precursors under thermally promoted, metal-free conditions and highlights the unique reactivity profile of B_2neop_2 relative to more commonly used diboron reagents such as B_2pin_2 and B_2cat_2. The radical borylation strategy has been demonstrated primarily on primary and secondary alkyl sulfones, with tertiary alkyl and aryl substrates remaining untested. A gram-scale (5 mmol)

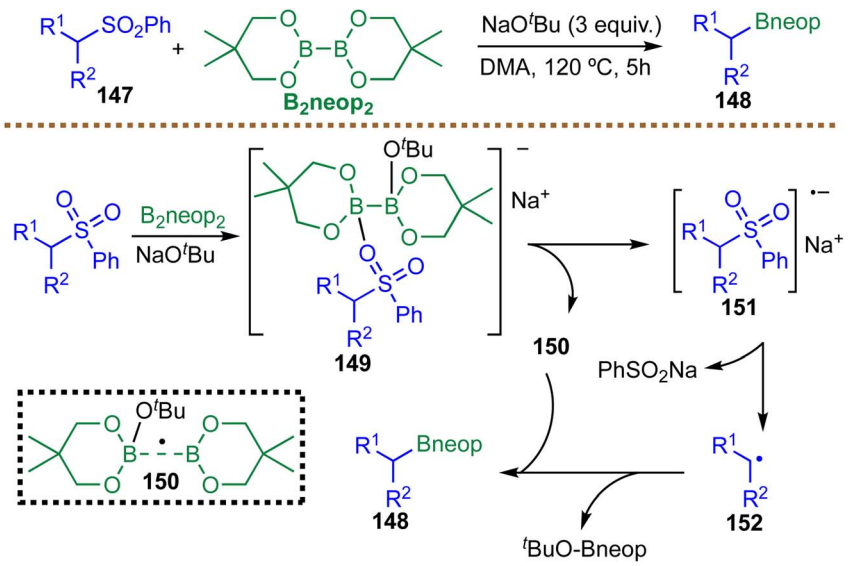

Scheme 35 Base-mediated radical borylation of alkyl sulfones.

borylation of 4-fluorophenyl sulfone under standard conditions afforded the corresponding boronic ester in 72% yield, only modestly lower than the 85% yield observed on a 0.5 mmol scale.[130] This result indicates that the method retains good efficiency upon scale-up despite its currently limited substrate scope.

Expanding the toolkit for metal-free radical borylation, Mo and co-workers also demonstrated in 2021 a light- and transition-metal-free protocol for the borylation of alkyl bromides and iodides employing tris(trimethylsilyl)silane (TTMSS) and B_2cat_2 (Scheme 36).[133] The method operates under neutral conditions and tolerates diverse functional groups, efficiently converting primary, secondary, and tertiary alkyl halides into alkyl boronic esters in moderate to good yields. Mechanistic investigations, including TEMPO-trapping, radical clock experiments, and DFT calculations, support a classical radical pathway. Radical initiation occurs *via* AIBN-mediated generation of silyl radicals from TTMSS, which abstract halogens from alkyl bromides or iodides to form carbon-centered radicals. These alkyl radicals then add to B_2cat_2, generating a boryl radical intermediate that fragments to furnish the alkyl boronic esters. Computational analysis revealed that C–Br bond cleavage by the silyl radical is energetically favorable, while the subsequent radical addition to B_2cat_2 has a low activation barrier. The cycle is thermodynamically sustained through regeneration of B_2cat_2 and DMA. This work highlights how silane-mediated halogen abstraction can be harnessed to enable efficient, metal- and light-free radical borylation of alkyl halides. However, the requirement for stoichiometric amounts of the radical mediator TTMSS and the initiator AIBN, along with the formation of by-products from AIBN decomposition and silane consumption, limits the method's practicality for large-scale or industrial applications.

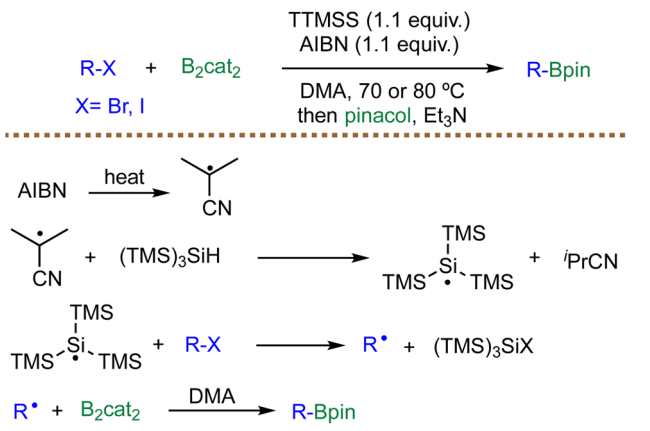

Scheme 36 Radical borylation of alkyl bromides and iodides using silane.

While Mo's protocol necessitates glovebox handling,[133] a more operationally straightforward approach was recently reported by Ogawa and co-workers, who developed a thermally driven method for generating aryl radicals from triarylbismuthines under open-air conditions (Scheme 37).[134] The strategy exploits the relatively weak Ar–Bi bond, which undergoes thermal homolysis facilitated by atmospheric oxygen. Mechanistic studies support a radical pathway: the reaction is completely suppressed under an argon atmosphere and is significantly inhibited by the radical scavenger TEMPO, which also successfully traps the phenyl radical to form the TEMPO–Ph adduct. The authors propose a dual activation mechanism in which oxygen acts as a radical initiator. The resulting aryl radical is then trapped by B_2pin_2, likely proceeding *via* two competing pathways: direct addition to B_2pin_2 (Path A) or trapping by a pinB$^\bullet$ radical generated through oxygen-mediated homolysis of the B–B bond in B_2pin_2 (Path B). This method is notable for its operational simplicity, requiring only heating in air, and affords aryl boronic esters in moderate to good yields. However, certain substrates—such as tri(*p*-

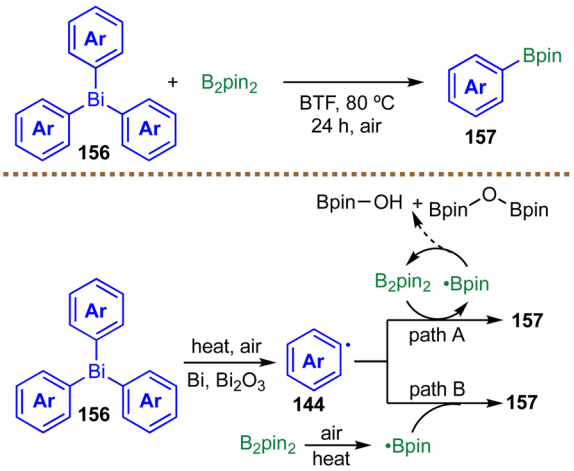

Scheme 37 Synthesis of arylboronates *via* thermal generation of aryl radicals.

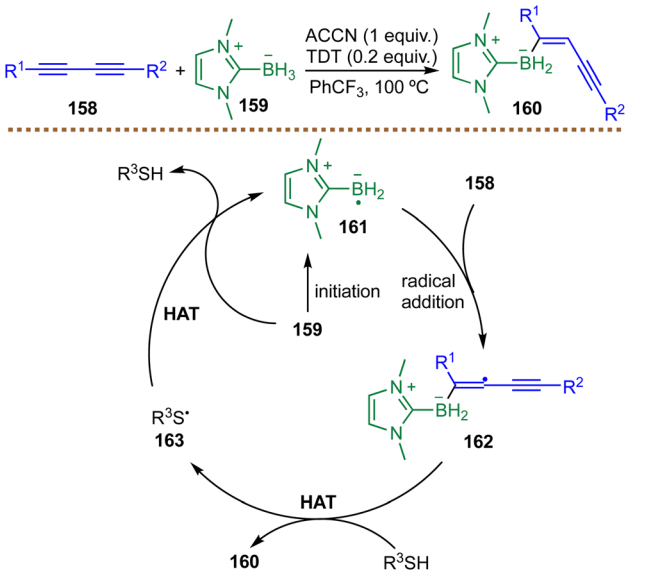

Scheme 38 Radical *trans*-hydroboration of substituted 1,3-diynes.

fluorophenyl)bismuthine and tri(1-naphthyl)bismuthine—exhibit low solubility in the chosen solvent [benzotrifluoride (BTF)], leading to poor conversion and diminished yields. This limitation underscores the importance of sufficient precursor solubility to enable efficient radical generation and productive C–B bond formation.

While previous methods generate carbon-centered radicals for subsequent borylation, an alternative strategy leverages the direct generation and reactivity of boryl radicals. A representative example is the radical *trans*-hydroboration of diynes reported by Taniguchi and co-workers. In 2021, Taniguchi *et al.* developed a metal-free, radical-based strategy for the highly stereoselective *trans*-hydroboration of 1,3-diynes using an N-heterocyclic carbene borane **159** (Scheme 38).[135] The reaction is initiated by thermal decomposition of an azo initiator (ACCN or AIBN), generating radicals that abstract a hydrogen atom from the thiol catalyst *tert*-dodecanethiol (TDT) to form a thiyl radical **163**. This thiyl radical **163** then engages in a polarity-reversal catalysis (PRC) step, abstracting a hydrogen atom from **159** to generate the key nucleophilic NHC-boryl radical **161**. This boryl radical **161** adds regioselectively to the 1,3-diyne substrate **158**, forming a vinyl radical intermediate **162**. The high *trans*-selectivity arises in the subsequent chain-carrying step, in which the vinyl radical **162** abstracts hydrogen from the thiol catalyst with high stereocontrol, delivering the (*E*)-alkenyl boron product **160** and regenerating the thiyl radical **163**. Notably, the need for thiol-mediated PRC distinguishes this chemistry from their earlier work on aryl alkynes, highlighting how the electronic properties of the conjugated diyne system modulate the HAT step. Overall, this method offers an efficient entry to otherwise difficult-to-access (*E*)-borylated enynes with excellent regio- and stereoselectivity. The protocol performs reliably for 1,3-diynes bearing *n*-alkyl and *c*-alkyl substituents and selected silyl and propargyl-ether groups. However, attempts to apply the standard conditions to diaryl diynes, for example, 1,4-diphenylbuta-1,3-diyne, resulted in complex product mixtures rather than the desired *trans*-hydroboration product. The authors attribute this limitation to differences in hydrogen-atom-transfer (HAT) rates between aryl and alkyl/silyl substituents, which disrupt the selectivity of the radical chain process. Moreover, the study does not systematically explore electronically biased aryl substrates (electron-rich or strongly electron-withdrawing), heteroaryl systems, or sterically demanding substituents. Consequently, the method's tolerance toward pronounced electronic and steric variation remains to be established.

3.4 Miscellaneous metal-free radical borylations

A final set of emerging methodologies occupies a hybrid space that does not fall neatly into classical thermal, photochemical, or electrochemical categories. One notable example is the recent work by Xia and co-workers, who developed a metal- and oxidant-free photoelectrochemical strategy for C(sp^3)–H borylation of unactivated hydrocarbons (Scheme 39).[136] The process merges the strengths of electrochemistry and photochemistry to achieve controlled radical generation under mild conditions. In this system, chloride ions undergo anodic oxidation to form Cl_2, which is subsequently cleaved under visible light to generate chlorine radicals. These radicals initiate HAT from C(sp^3)–H bonds, furnishing alkyl radicals **165** or **166**. Mechanistic studies, including cyclic voltammetry, kinetic isotope effect measurements, radical trapping experiments, and competition studies, revealed that HAT is both fast and reversible. Although chlorine radicals preferentially abstract hydrogen from tertiary C–H bonds, steric constraints in the subsequent radical coupling step bias the system toward primary radical capture by B_2cat_2, resulting in an unusual distal methyl selectivity.

Two mechanistic pathways were proposed: (i) direct HAT mediated by free chlorine radicals, followed by trapping of the resulting alkyl radical by $B_2(cat)_2$ and (ii) an alternative path involving a Cl–boron "ate" complex **171** that can also mediate HAT. Meanwhile, protons are reduced to H_2 at the cathode, eliminating the need for sacrificial oxidants and allowing the reaction to proceed cleanly. Collectively, this study illustrates

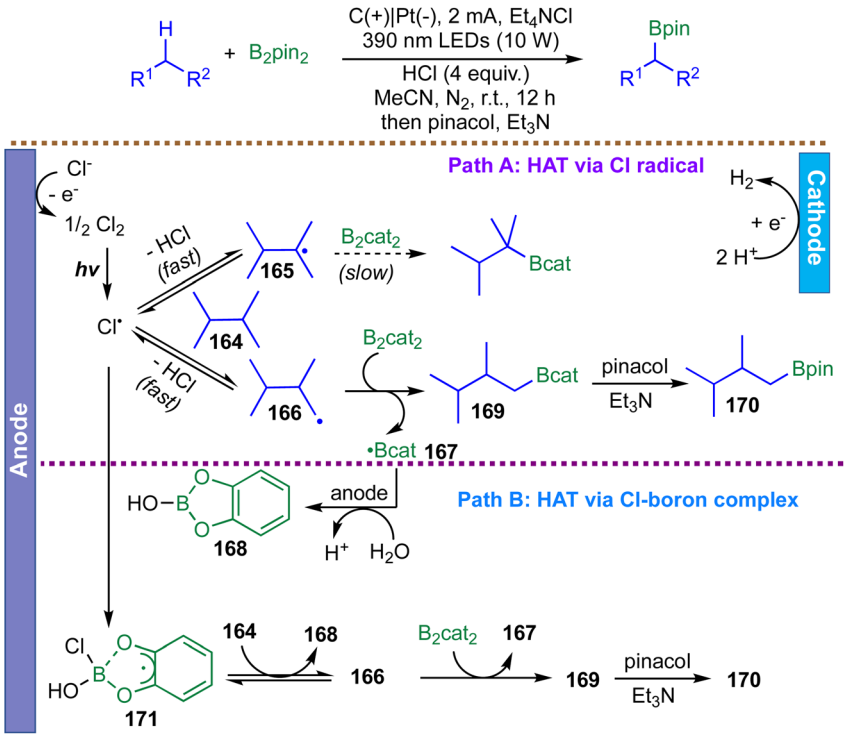

Scheme 39 Photoelectrochemical oxidative C(sp^3)–H borylations.

how synergistic photoelectrochemical activation provides control over radical formation and capture, enabling site-selective C–H borylation. While the transformation is broadly compatible with alkanes, halides, silanes, ketones, and nitriles, the authors explicitly note that nitrogen-containing substrates, including amines, amides, and sulfonamides, are poorly tolerated. This limitation markedly constrains the method's applicability to pharmaceutically relevant scaffolds and other biologically significant molecules, which frequently incorporate nitrogen-based functionalities. The protocol is, however, amenable to scale-up: a 10 mmol batch reaction furnished the desired product in 52% yield (1.25 g), and further adaptation to continuous-flow conditions (10 mA, 390 nm LEDs, 0.1 mL min^{-1}) enabled a 20 mmol preparation in 61% yield.[136]

Mechanochemistry has recently emerged as an unconventional yet powerful platform for radical generation, expanding the toolbox beyond photochemical and electrochemical paradigms. In this context, Yu and co-workers demonstrated that aryldiazonium tetrafluoroborates undergo direct mechanically induced C–N bond homolysis in the presence of NaCl, enabling the generation of aryl radicals under solvent- and metal-free ball-milling conditions (Scheme 40).[137] In this study, the borylation of aryldiazonium tetrafluoroborates represents only a minor component of the overall work, with merely two examples demonstrated to yield 4-methoxyphenyl-Bpin and 4-chlorophenyl-Bpin in 62% and 52% yield, respectively. The extremely limited substrate scope leaves the generality of this ball-milling-enabled radical borylation largely untested, and future expansion to a broader range of aryl diazonium salts will be essential to assess the robustness and synthetic utility of this mechanochemical approach.

Mechanistic investigations provide compelling evidence that the mechanochemical borylation of aryldiazonium salts proceeds through a force-mediated radical pathway, rather than through thermal, photochemical, or redox activation. Several complementary experiments support this conclusion. First, temperature monitoring during ball milling shows only modest heating (<40 °C), far below the threshold required for thermal homolysis. Control reactions performed without milling yield no detectable product, and the reaction remains efficient even in the absence of redox-active additives, collectively excluding both thermal and electron-transfer initiation. Second, radical trapping experiments using TEMPO or 1,1-diphenylethylene markedly suppress product formation and afford isolable adducts, directly confirming the generation of aryl radicals under milling conditions. Third, PXRD analysis reveals the *in situ* formation of aryldiazonium chlorides through

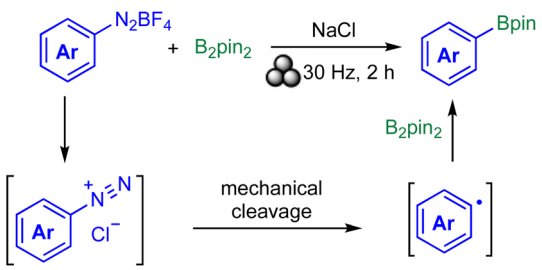

Scheme 40 Borylation of aryldiazonium salts by ball milling.

mechanically induced anion exchange between aryldiazonium tetrafluoroborates and NaCl. As aryldiazonium chlorides are significantly more prone to homolysis, their appearance correlates closely with product formation, indicating that they serve as the operative radical precursors. Finally, systematic variation of milling parameters demonstrates a clear positive correlation between mechanical energy input and reaction efficiency: higher milling frequencies and greater impact energies lead to faster reactions and higher yields. This relationship underscores that mechanical force—through high-energy impacts that generate localized stress and lattice disruption—is responsible for initiating C–N bond homolysis. Within this framework, NaCl fulfills a dual mechanistic role by promoting anion exchange to generate the more labile diazonium chlorides and by participating in their force-driven fragmentation.[137]

Notably, the authors contextualize mechanochemical radical borylation within the broader landscape of radical chemistry. The underlying rationale of this approach is that mechanical energy—delivered through high-frequency ball milling—can directly induce homolytic cleavage of suitably activated bonds, such as the C–N bond in aryldiazonium salts, without requiring heat, light, or redox reagents.[137] Compared with photochemical initiation, which depends on light absorption and EDA complex formation, mechanochemistry generates radicals independent of substrate optical properties, circumventing challenges such as photobleaching, limited light penetration, or competing photophysical processes. This mechanistic distinction underscores the unique advantages of force-mediated activation, providing a complementary, operationally simple, and potentially scalable platform for aryl radical borylation and other radical transformations.

4. Synthetic applications of metal-free radical borylations

Metal-free radical borylation has rapidly evolved from a methodological curiosity into a powerful and practical tool for complex-molecule synthesis and late-stage functionalization. Early studies demonstrated that simple radical precursors such as alkyl or aryl iodides, bromides, and other suitable substrates can be converted into the corresponding boronic esters under metal-free conditions using commercially available diboron reagents. This advance obviates the need for transition-metal catalysts while maintaining broad functional-group tolerance. These protocols provide a straightforward entry to boronic esters that are readily amenable to downstream cross-couplings and derivatizations, enhancing their utility in multi-step synthetic sequences and complex-molecule construction.

A key synthetic advantage of metal-free radical borylation lies in its utility for late-stage functionalization, particularly for complex natural products and pharmaceutical intermediates. Photoinduced C(sp^3)–H borylation *via* hydrogen atom transfer has emerged as a straightforward approach for modifying API and bioactive molecules. For example, Mo *et al.* demonstrated the tertiary C(sp^3)–H borylation of lithocholic acid, highlighting the method's utility in the selective functionalization of complex steroidal frameworks.[93] Similarly Guo and Xia *et al.* developed a photoelectrochemical strategy that enabled site-selective C–H borylation of squalene[136] (Scheme 41), showcasing the potential for controlled radical formation and distal methyl-selective functionalization. Importantly, both strategies have been validated for scalability. Mo *et al.* carried out gram-scale borylation on a 10 mmol scale, affording the corresponding boronic ester in 59% yield (1.75 g) compared to 73% yield on a 0.3 mmol scale.[93] In parallel, Guo and Xia *et al.* scaled their photoelectrochemical borylation in batch to 10 mmol (52% yield, 1.25 g) and further translated the protocol to continuous-flow operation (I = 10 mA, 390 nm LEDs, 0.1 mL min^{-1}), achieving 61% yield on a 20 mmol scale.[136] These examples underscore the practicality and robustness of metal-free radical borylation; however, detailed process metrics, such as space–time yields, *E*-factors, and long-term flow stability, remain largely unreported. Addressing these gaps will be an important direction for future development.

Complementing advances in C(sp^3)–H borylation, recent studies have also expanded metal-free radical borylation to heteroarenes and aliphatic amines, addressing long-standing challenges in site-selective functionalization. In 2021, Leonori and co-workers reported a photocatalytic strategy for the site-selective C–H borylation of azines using stable and inexpensive amine-borane reagents (Scheme 42A).[67] The approach leverages the coordination of the amine to the boron center, forming a Lewis acid–base adduct that facilitates hydrogen atom transfer to generate a highly nucleophilic boryl radical. This open-shell species selectively adds to the C2-position of protonated N-heteroaromatics, a site typically resistant to conventional functionalization. This metal-free radical pathway enables access to a wide array of structurally complex and

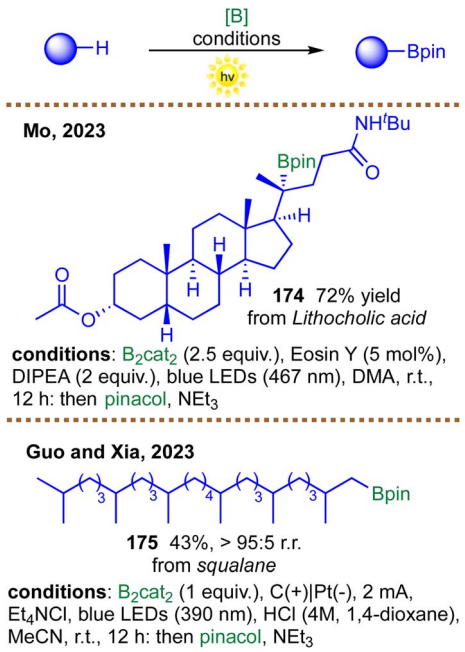

Scheme 41 Application of photochemical C(sp^3)–H borylation on natural products.

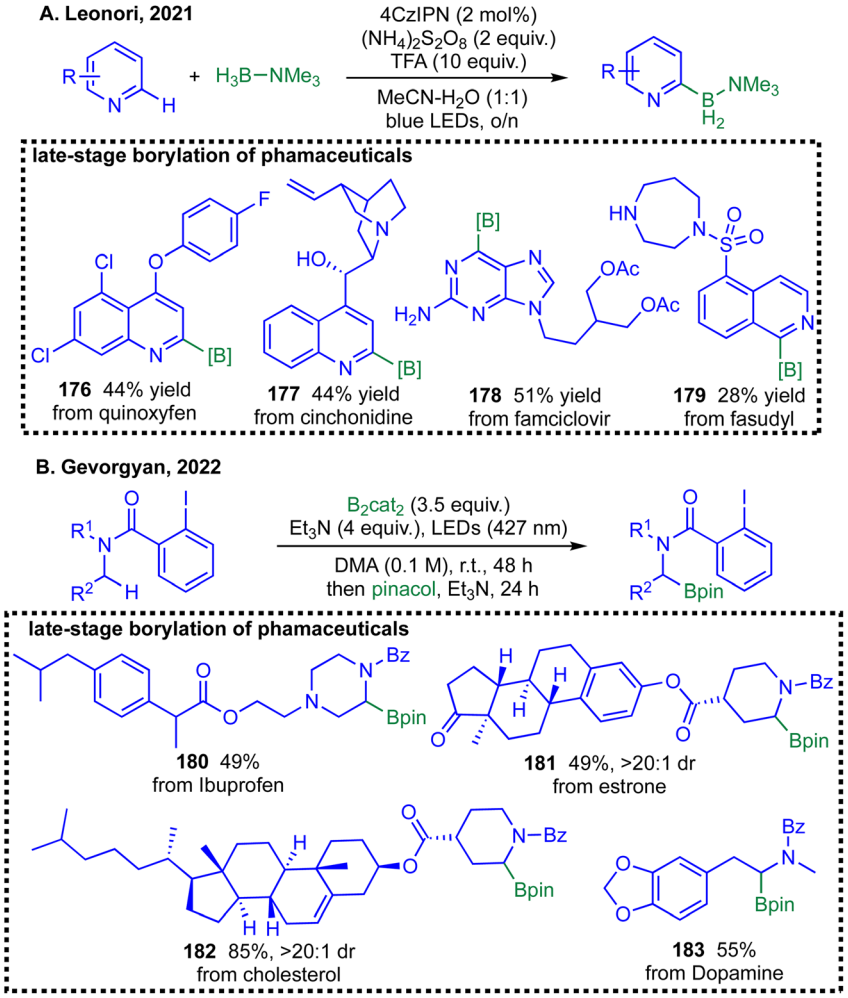

Scheme 42 Photoinduced C–H borylations and their synthetic applications; (A) C–H borylations by Leonori *et al.* in 2021 and its synthetic applications; (B). C–H borylations by Gevorgyan *et al.* in 2022 and its late-stage applications.

industrially relevant molecules, including pharmaceutical agents and agrochemical derivatives (**176–179**).

Building on this concept, Gevorgyan *et al.* developed in 2022 a general and selective metal-free method for the radical α-C–H borylation of aliphatic amines (Scheme 42B).[91] The strategy employs a commercially available 2-iodobenzoyl group as a radical translocating group, which is easily installed and removed. This protocol has been successfully applied to the late-stage functionalization of pharmaceutically relevant amines, including derivatives of ibuprofen (**180**), estrone (**181**), cholesterol (**182**), dopamine (**183**), and drug fragments from serotonin antagonists and antihistamines.

Collectively, these studies illustrate how metal-free radical borylation can be harnessed for selective C–H functionalization across both heteroaromatic and aliphatic substrates, significantly broadening the synthetic toolkit for complex molecule modification.

Expanding the toolbox of metal-free borylation, recent electrochemical strategies have enabled new bond disconnections by leveraging naturally occurring functional groups as synthetically versatile handles. Lin *et al.* reported a unified electroreductive deoxygenative borylation of alcohols, aldehydes, and ketones (Scheme 43A).[121] This approach permits the direct conversion of ubiquitous carbonyl and hydroxyl functionalities into valuable boronic esters, enabling late-stage diversification of structurally complex scaffolds, including celestolide, desoxyanisoin, podophyllotoxin, and donepezil.

In a complementary strategy, Lundberg *et al.* reported an electrochemical desulfurative borylation of thioethers that similarly enables late-stage installation of boron from readily available sulfide precursors (Scheme 43B).[123] This method has been applied to a range of pharmaceuticals and natural products, such as terfenadine, roflumilast, diphenidol, and rosuvastatin precursor, highlighting its synthetic utility. A gram-scale demonstration using benzyl(phenyl)sulfane afforded benzyl Bpin in 77% yield (1 g, 6 mmol scale) under modified conditions (3 equiv Hbpin in MeCN), though this represents a notable decrease from the 95% yield obtained on a 0.5 mmol scale. This disparity underscores a key challenge: while these electrochemical borylations are highly effective on a small scale, translation to the preparative scale remains nontrivial.

Together, these electrochemical deoxygenative and desulfurative platforms offer powerful and mild metal-free routes to

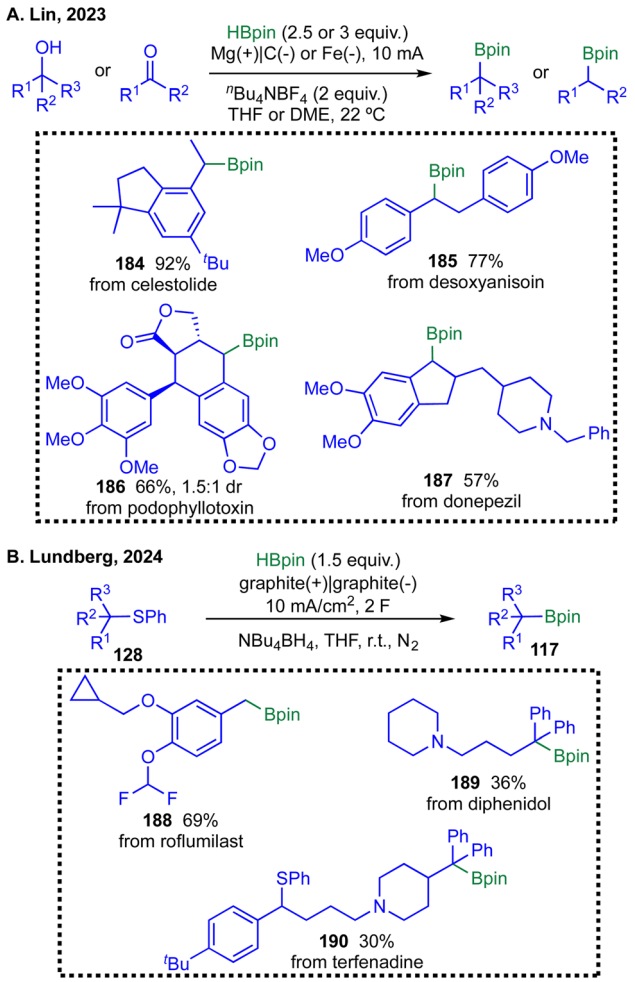

Scheme 43 Electrochemical radical borylations and their synthetic applications; (A) electrochemical borylations by Lin *et al.* in 2023 and its late-stage applications; (B) electrochemical borylations by Lundbeg *et al.* in 2024 and its synthetic applications.

boron-containing building blocks from abundant feedstock chemicals. However, improving scalability and operational robustness will be an important next step for broad adoption in synthesis and process chemistry.

5. Summary and outlook

This review has outlined the remarkable evolution of metal-free radical borylation, a field that has progressed from a conceptual curiosity to a powerful and broadly applicable synthetic platform. We summarized the fundamental mechanistic principles underpinning the generation of alkyl, aryl, and boryl radicals and provided a systematic overview of the diverse catalytic modalities that enable these transformations, including photoinduced (SET, EDA, HAT, and EnT), electrochemical, and thermal strategies. Collectively, these approaches address several longstanding limitations of transition-metal catalysis by offering enhanced functional-group compatibility, eliminating concerns over metal residues, and enabling distinct regiochemical outcomes. Notably, some metal-free radical protocols deliver otherwise inaccessible selectivity patterns, such as contra-thermodynamic[67] or contra-steric C(sp^3)–H borylation,[93] underscoring their unique strategic value in modern synthesis. The synthetic utility of these developments is profound. Metal-free radical borylation has emerged as a powerful tool for late-stage functionalization of complex molecules, including pharmaceuticals, natural products, and agrochemicals, enabling the installation of valuable boron handles that serve as gateways to further diversification through cross-coupling and related transformations.

Despite these significant advances, several challenges and opportunities for future research remain:

5.1. C(sp^3)–H borylation

While impressive strides have been made, achieving predictable, site-selective borylation of unactivated, aliphatic C–H bonds, particularly in the presence of multiple similar sites, remains a formidable challenge. The development of catalysts or directing strategies that can override innate bond strength and steric biases to achieve programmable selectivity is a key frontier.[138–140]

5.2. Stereocontrol

While progress has been made in achieving regioselectivity,[67,93,141,142] the control of absolute stereochemistry in radical borylation remains in its infancy. Future opportunities lie in the development of chiral Lewis base catalysts, enantioselective HAT systems, and stereocontrolled radical-trapping strategies, which could unlock asymmetric pathways to enantioenriched alkyl boronic esters—high-value motifs with significant relevance in medicinal chemistry.

5.3. Atom economy and sustainability

Although metal-free radical borylation protocols circumvent the use of metals and eliminate concerns about metal contamination, several sustainability challenges remain. Many current methods require excess bases or additives, stoichiometric amounts of diboron reagents, prefunctionalized substrates, and strict exclusion of oxygen or moisture. These factors diminish the overall atom and step economy, complicate reaction handling, and limit the practicality of these methods in industrial settings.[143,144] Future efforts should prioritize the development of atom-economical, operationally robust, and ideally aerobic radical borylation strategies that employ simple, non-prefunctionalized substrates and are readily scalable for large-scale applications. Moreover, the development of systematic evaluation metrics, such as space–time yields and *E*-factors, to assess the sustainability of these methods is highly desirable.

5.4. Scalability

Although several photoinduced and electrochemical radical borylation protocols exhibit excellent reactivity on a small scale, their performance often diminishes upon translation to multigram quantities, necessitating additional optimization.[123] Scaling these methods further to the kilogram scale or to continuous-flow processes introduces additional challenges, as

photoreactors or electrolysis setups typically require substantial redesign to ensure uniform light penetration or efficient mass/electron transfer. Taken together, careful investigation of scale-dependent factors and the development of robust batch and continuous-flow platforms represent essential next steps for advancing the practical implementation of radical borylation chemistry.

5.5. Mechanistic understanding and prediction

As the complexity of catalytic systems grows (*e.g.*, dual photoredox/HAT and ConPET), so does the need for deep mechanistic insight. Advanced spectroscopic techniques, *in situ* monitoring, and computational modeling will be crucial for deciphering complex catalytic cycles, identifying key intermediates, and rationally designing next-generation systems with predictable reactivity.[145,146]

5.6. Integration with emerging technologies

The convergence of metal-free borylation with other cutting-edge technologies offers compelling opportunities for future innovation. Notable directions include the development of electrosynthetic platforms for scalable, redox-neutral transformations; the application of mechanochemistry to enable solvent-free radical generation; and the use of machine learning to navigate complex reaction parameter spaces, accelerate optimization, and predict suitable conditions for new substrates.[147–150]

In conclusion, metal-free radical borylation has evolved into a robust and strategically significant platform for constructing organoboron compounds, offering reactivity and selectivity profiles that complement those of traditional metal-based methods. Yet, realizing its full potential will require concerted efforts across several key fronts. Achieving predictable and programmable C(sp^3)–H borylation, particularly for unactivated aliphatic frameworks, remains a central challenge, calling for catalysts or directing strategies that can selectively override innate steric and bond-strength biases. Likewise, the development of asymmetric variants lags behind other areas of radical chemistry, highlighting the need for chiral Lewis bases, enantioselective HAT catalysts, and stereocontrolled trapping processes capable of delivering enantioenriched boron-containing motifs.

Improving atom economy and operational sustainability is equally essential, driving the need for protocols that reduce auxiliary reagents, avoid prefunctionalized substrates, and operate reliably under aerobic conditions. In parallel, achieving practical scalability, from multigram synthesis to continuous-flow or even kilogram-scale production, will require systematic investigation of light penetration, mass transport, and reactor engineering for both photochemical and electrochemical platforms. Furthermore, deeper mechanistic insight, supported by modern spectroscopic tools, computational modeling, and *in situ* monitoring, will be crucial for unraveling complex catalytic manifolds such as dual photoredox/HAT or ConPET systems, ultimately guiding the rational design of next-generation catalysts.

Finally, the integration of metal-free borylation with emerging technologies such as electrosynthesis, mechanochemistry, and data-driven reaction optimization offers transformative potential for improving efficiency, sustainability, and predictability. By addressing these specific challenges, the field is well positioned to expand its practical impact and to solidify metal-free radical borylation as a core strategy for constructing complex, functionalized organoboron architectures in both academic and industrial settings.

Author contributions

Z. Q. and B. W. prepared the manuscript with contributions from all the co-authors. All authors revised the manuscript.

Conflicts of interest

The authors declare no conflict of interest.

Data availability

No new data were generated in this review. All data analyzed in this study are from the publicly available literature and can be found in the reference list.

Acknowledgements

This research was financially supported by the National Natural Science Foundation of China (Grant No. 21868011), the National Key R&D Program of China (Grant No. 2017YFC1103800), the Shandong Provincial Natural Science Foundation (Grant No. ZR2024QB243) and the Talent Youth Program of Shandong University of Science and Technology.

References

1 J. W. B. Fyfe and A. J. B. Watson, *Chem*, 2017, **3**, 31–55.
2 R. J. Grams, W. L. Santos, I. R. Scorei, A. Abad-García, C. A. Rosenblum, A. Bita, H. Cerecetto, C. Viñas and M. A. Soriano-Ursúa, *Chem. Rev.*, 2024, **124**, 2441–2511.
3 C. Diner and K. J. Szabó, *J. Am. Chem. Soc.*, 2017, **139**, 2–14.
4 J. Carreras, A. Caballero and P. J. Pérez, *Chem.–Asian J.*, 2019, **14**, 329–343.
5 J. Ding, T. Rybak and D. G. Hall, *Nat. Commun.*, 2014, **5**, 5474.
6 B. C. Das, P. Thapa, R. Karki, C. Schinke, S. Das, S. Kambhampati, S. K. Banerjee, P. Van Veldhuizen, A. Verma, L. M. Weiss and T. Evans, *Future Med. Chem.*, 2013, **5**, 653–676.
7 M. P. Silva, L. Saraiva, M. Pinto and M. E. Sousa, *Molecules*, 2020, **25**, 4323.
8 K. Messner, B. Vuong and G. K. Tranmer, *Pharmaceuticals*, 2022, **15**, 264.
9 S. P. Thomas, R. M. French, V. Jheengut and V. K. Aggarwal, *Chem. Rec.*, 2009, **9**, 24–39.
10 Y. Jiang and S. E. Schaus, *Angew. Chem., Int. Ed.*, 2017, **129**, 1566–1570.

11 D. S. Barnett, P. N. Moquist and S. E. Schaus, *Angew. Chem., Int. Ed.*, 2009, **48**, 8679–8682.
12 H. T. P. Pham, S. Bhatt and K. L. Hull, *ACS Catal.*, 2025, **15**, 14564–14574.
13 J. Marco-Martínez, E. Buñuel, R. López-Durán and D. J. Cárdenas, *Chem.–Eur. J.*, 2011, **17**, 2734–2741.
14 P. Zhang, I. A. Roundtree and J. P. Morken, *Org. Lett.*, 2012, **14**, 1416–1419.
15 Z. Quan, Y. Liu, A. Zhen, F. Ma, X. Gao, J. Sun and B. Wang, *Eur. J. Org Chem.*, 2025, **00**, e202500319.
16 C. Haldar, M. E. Hoque, J. Chaturvedi, M. M. M. Hassan and B. Chattopadhyay, *Chem. Commun.*, 2021, **57**, 13059–13074.
17 T. Yamamoto, A. Ishibashi and M. Suginome, *Org. Lett.*, 2019, **21**, 6235–6240.
18 M. L. Sall, A. K. D. Diaw, D. Gningue-Sall, S. E. Aaron and J.-J. Aaron, *Environ. Sci. Pollut. Res.*, 2020, **27**, 29927–29942.
19 H. K. Okoro, M. M. Orosun, F. A. Oriade, T. M. Momoh-Salami, C. O. Ogunkunle, A. G. Adeniyi, C. Zvinowanda and J. C. Ngila, *Sustainability*, 2023, **15**, 6974.
20 Z. Bahmani, R. Nabizadeh, K. Yaghmaeian and M. Yunesian, *Sci. Rep.*, 2025, **15**, 6395.
21 J. H. Docherty, T. M. Lister, G. Mcarthur, M. T. Findlay, P. Domingo-Legarda, K. Jacob, S. Choudhary and I. Larrosa, *Chem. Rev.*, 2023, **123**, 7692–7760.
22 E. Lalik, R. Kosydar, R. Tokarz-Sobieraj, M. Witko, T. Szumełda, M. Kołodziej, W. Rojek, T. Machej, E. Bielańska and A. Drelinkiewicz, *Appl. Catal., A*, 2015, **501**, 27–40.
23 S.-H. Ryu, G. Kim, S. Gupta, S. Bhattacharjee, S.-C. Lee, H. Lee, J.-H. Choi and H. Jeong, *Chem. Eng. J.*, 2024, **485**, 149487.
24 M. Häring, A. Abramov, K. Okumura, I. Ghosh, B. König, N. Yanai, N. Kimizuka and D. Díaz Díaz, *J. Org. Chem.*, 2018, **83**, 7928–7938.
25 A. J. Sicard and R. T. Baker, *Org. Process Res. Dev.*, 2020, **24**, 2950–2952.
26 Z.-H. Shang, J. Pan, Z. Wang, Z.-X. Zhang and J. Wu, *Eur. J. Org Chem.*, 2023, **26**, e202201379.
27 J. R. Coombs, R. A. Green, F. Roberts, E. M. Simmons, J. M. Stevens and S. R. Wisniewski, *Organometallics*, 2019, **38**, 157–166.
28 N. Ishiwata, T. Komuro, K. Takahashi, Y. Zenzai, H. Tobita and H. Hashimoto, *Chem.–Asian J.*, 2025, **20**, e00709.
29 K. Chen, L. Wang, G. Meng and P. Li, *Synthesis*, 2017, **49**, 4719–4730.
30 K. K. Das, S. Paul and S. Panda, *Org. Biomol. Chem.*, 2020, **18**, 8939–8974.
31 Y.-M. Tian, X.-N. Guo, H. Braunschweig, U. Radius and T. B. Marder, *Chem. Rev.*, 2021, **121**, 3561–3597.
32 L. Luo, S. Tang, J. Wu, S. Jin and H. Zhang, *Chem. Rec.*, 2023, **23**, e202300023.
33 D. Ravelli, S. Protti and M. Fagnoni, *Chem. Rev.*, 2016, **116**, 9850–9913.
34 K. Grudzień, A. Zlobin, J. Zadworny, K. Rybicka-Jasińska and B. Sadowski, *Org. Chem. Front.*, 2024, **11**, 5232–5277.
35 A. B. Waghamare, R. K. Raut, N. Patel and M. Majumdar, *Eur. J. Inorg. Chem.*, 2022, e202200089.
36 J. Klett, Ł. Woźniak and N. Cramer, *Angew. Chem., Int. Ed.*, 2022, **61**, e202202306.
37 R. D. Riley, B. S. N. Huchenski, K. L. Bamford and A. W. H. Speed, *Angew. Chem., Int. Ed.*, 2022, **61**, e202204088.
38 A. M. Mfuh, V. T. Nguyen, B. Chhetri, J. E. Burch, J. D. Doyle, V. N. Nesterov, H. D. Arman and O. V. Larionov, *J. Am. Chem. Soc.*, 2016, **138**, 8408–8411.
39 K. Chen, M. S. Cheung, Z. Lin and P. Li, *Org. Chem. Front.*, 2016, **3**, 875–879.
40 K. Chen, S. Zhang, P. He and P. Li, *Chem. Sci.*, 2016, **7**, 3676–3680.
41 A. M. Mfuh, J. D. Doyle, B. Chhetri, H. D. Arman and O. V. Larionov, *J. Am. Chem. Soc.*, 2016, **138**, 2985–2988.
42 J. G. Hernández, *Beilstein J. Org. Chem.*, 2017, **13**, 1463–1469.
43 X. Qi, H.-P. Li, J.-B. Peng and X.-F. Wu, *Tetrahedron Lett.*, 2017, **58**, 3851–3853.
44 H. B. Chandrashekar, A. Maji, G. Halder, S. Banerjee, S. Bhattacharyya and D. Maiti, *Chem. Commun.*, 2019, **55**, 6201–6204.
45 S. Zhu, J. Yan, Y. Zhou, K. Yang and Q. Song, *Green Synth. Catal.*, 2021, **2**, 299–302.
46 J. Lalevée and J. P. Fouassier, Overview of Radical Initiation, in *Encyclopedia of Radicals in Chemistry, Biology and Materials*, John Wiley & Sons, Ltd, 2012.
47 B. Schweitzer-Chaput, E. Boess and M. Klussmann, *Org. Lett.*, 2016, **18**, 4944–4947.
48 M. Yan, J. C. Lo, J. T. Edwards and P. S. Baran, *J. Am. Chem. Soc.*, 2016, **138**, 12692–12714.
49 L. Zhang and L. Jiao, *J. Am. Chem. Soc.*, 2017, **139**, 607–610.
50 T. Wan, L. Capaldo, D. Ravelli, W. Vitullo, F. J. de Zwart, B. de Bruin and T. Noël, *J. Am. Chem. Soc.*, 2023, **145**, 991–999.
51 X. Chen, X. Zhou, J. He and X. Liu, *Synthesis*, 2025, **57**, 2539–2550.
52 S.-H. Ueng, A. Solovyev, X. Yuan, S. J. Geib, L. Fensterbank, E. Lacôte, M. Malacria, M. Newcomb, J. C. Walton and D. P. Curran, *J. Am. Chem. Soc.*, 2009, **131**, 11256–11262.
53 T. Taniguchi, *Chem. Soc. Rev.*, 2021, **50**, 8995–9021.
54 H. Zheng, H. Lu, C. Su, R. Yang, L. Zhao, X. Liu and H. Cao, *Chin. J. Chem.*, 2023, **41**, 193–198.
55 F. Mo, Y. Jiang, D. Qiu, Y. Zhang and J. Wang, *Angew. Chem., Int. Ed.*, 2010, **49**, 1846–1849.
56 D. Qiu, L. Jin, Z. Zheng, H. Meng, F. Mo, X. Wang, Y. Zhang and J. Wang, *J. Org. Chem.*, 2013, **78**, 1923–1933.
57 D. Leifert and A. Studer, *Angew. Chem., Int. Ed.*, 2020, **59**, 74–108.
58 A. Ruffoni, R. C. Mykura, M. Bietti and D. Leonori, *Nat. Synth.*, 2022, **1**, 682–695.
59 J. Qi, F.-L. Zhang, J.-K. Jin, Q. Zhao, B. Li, L.-X. Liu and Y.-F. Wang, *Angew. Chem., Int. Ed.*, 2020, **59**, 12876–12884.
60 A. Velloth, P. Kumar, S. Butt and S. Venkataramani, *Asian J. Org. Chem.*, 2025, **14**, e202400686.
61 D. Lai, S. Ghosh and A. Hajra, *Org. Biomol. Chem.*, 2021, **19**, 4397–4428.

62 V. D. Nguyen, V. T. Nguyen, S. Jin, H. T. Dang and O. V. Larionov, *Tetrahedron*, 2019, **75**, 584–602.
63 C. Lian, J. Zhang, D. Qiu and F. Mo, *Chin. J. Chem.*, 2025, **43**, 104–115.
64 L. Capaldo, D. Ravelli and M. Fagnoni, *Chem. Rev.*, 2022, **122**, 1875–1924.
65 C. Shu, A. Noble and V. K. Aggarwal, *Nature*, 2020, **586**, 714–719.
66 Q. Liu, L. Zhang and F. Mo, *Acta Chim. Sin.*, 2020, **78**, 1297.
67 J. H. Kim, T. Constantin, M. Simonetti, J. Llaveria, N. S. Sheikh and D. Leonori, *Nature*, 2021, **595**, 677–683.
68 L. Zhang, Z.-Q. Wu and L. Jiao, *Angew. Chem.*, 2020, **132**, 2111–2115.
69 L. Bai and L. Jiao, *Eur. J. Org Chem.*, 2024, **27**, e202400043.
70 A. Shiozuka, K. Sekine and Y. Kuninobu, *Org. Lett.*, 2021, **23**, 4774–4778.
71 S. Kubosaki, H. Takeuchi, Y. Iwata, Y. Tanaka, K. Osaka, M. Yamawaki, T. Morita and Y. Yoshimi, *J. Org. Chem.*, 2020, **85**, 5362–5369.
72 J. C. Herrera-Luna, D. Sampedro, M. C. Jiménez and R. Pérez-Ruiz, *Org. Lett.*, 2020, **22**, 3273–3278.
73 J. C. Herrera-Luna, D. D. Díaz, A. Abramov, S. Encinas, M. C. Jiménez and R. Pérez-Ruiz, *Org. Lett.*, 2021, **23**, 2320–2325.
74 J. Xu, J. Cao, X. Wu, H. Wang, X. Yang, X. Tang, R. Wei Toh, R. Zhou, E. W. L. Yeow and J. Wu, *J. Am. Chem. Soc.*, 2021, **143**, 13266–13273.
75 J.-K. Jin, F.-L. Zhang, Q. Zhao, J.-A. Lu and Y.-F. Wang, *Org. Lett.*, 2018, **20**, 7558–7562.
76 Y.-S. Huang, J. Wang, W.-X. Zheng, F.-L. Zhang, Y.-J. Yu, M. Zheng, X. Zhou and Y.-F. Wang, *Chem. Commun.*, 2019, **55**, 11904–11907.
77 H. Zheng, H. Lu, C. Su, R. Yang, L. Zhao, X. Liu and H. Cao, *Chin. J. Chem.*, 2023, **40**, 193–198.
78 J. Lu, Y. He, L. Ren, D. Li, X. Pan, L. Yang, J. Wang, S. Wei and J. Wei, *Synlett*, 2024, **35**, 1399–1404.
79 J. Wu, H. Wang, H. Fang, K. C. Wang, D. Ghosh, V. Fasano, A. Noble and V. K. Aggarwal, *J. Am. Chem. Soc.*, 2025, **147**, 19450–19457.
80 D. Kim and T. S. Teets, *Chem. Phys. Rev.*, 2022, **3**, 021302.
81 Z. Yang, Y. Liu, K. Cao, X. Zhang, H. Jiang and J. Li, *Beilstein J. Org. Chem.*, 2021, **17**, 771–799.
82 G. E. M. Crisenza, D. Mazzarella and P. Melchiorre, *J. Am. Chem. Soc.*, 2020, **142**, 5461–5476.
83 S. Wang, H. Wang and B. König, *Chem*, 2021, **7**, 1653–1665.
84 L. I. Panferova and A. D. Dilman, *Org. Lett.*, 2021, **23**, 3919–3922.
85 M. Li, S. Liu, H. Bao, Q. Li, Y.-H. Deng, T.-Y. Sun and L. Wang, *Chem. Sci.*, 2022, **13**, 4909–4914.
86 B. Li, K. Wang, H. Yue, A. Drichel, J. Lin, Z. Su and M. Rueping, *Org. Lett.*, 2022, **24**, 7434–7439.
87 Y. Wang, J. Dong, Y. Xiao, Z. Wang, W. Wu and D. Xue, *Org. Chem. Front.*, 2025, **12**, 4050–4057.
88 H. Cao, X. Tang, H. Tang, Y. Yuan and J. Wu, *Chem Catal.*, 2021, **1**, 523–598.
89 L. Capaldo and D. Ravelli, *Org. Lett.*, 2021, **23**, 2243–2247.
90 ak. L. Kuehn, L. Zapf, L. Werner, M. Stang, S. Würtemberger-Pietsch, I. Krummenacher, H. Braunschweig, E. Lacote, T. B. Marder and U. Radius, *Chem. Sci.*, 2022, **13**, 8321–8333.
91 S. Sarkar, S. Wagulde, X. Jia and V. Gevorgyan, *Chem*, 2022, **8**, 3096–3108.
92 J. He and S. P. Cook, *Chem. Sci.*, 2023, **14**, 9476–9481.
93 B. Sun, W. Li, Q. Liu, G. Zhang and F. Mo, *Commun. Chem.*, 2023, **6**, 156.
94 C. Wu, S. Luo, X. Liu and P. Liu, *Org. Chem. Front.*, 2024, **11**, 4785–4793.
95 F. Strieth-Kalthoff, M. J. James, M. Teders, L. Pitzera and F. Glorius, *Chem. Soc. Rev.*, 2018, **47**, 7190–7202.
96 E. A. Martynova, V. A. Voloshkin, S. G. Guillet, F. Bru, M. Beliš, K. Van Hecke, C. S. J. Cazin and S. P. Nolan, *Chem. Sci.*, 2022, **13**, 6852–6857.
97 K. Sun, C. Ge, X. Chen, B. Yu, L. Qu and B. Yu, *Nat. Commun.*, 2024, **15**, 9693.
98 J.-W. Li, T.-S. Duan, B. Sun and F.-L. Zhang, *Org. Biomol. Chem.*, 2024, **22**, 2819–2823.
99 S. Dutta, J. E. Erchinger, F. Strieth-Kalthoff, R. Kleinmansa and F. Glorius, *Chem. Soc. Rev.*, 2024, **53**, 1068–1089.
100 F. Wilkinson and A. A. Abdel-Shafi, *J. Phys. Chem. A*, 1999, **103**, 5425–5435.
101 F. Strieth-Kalthoff, M. J. James, M. Teders, L. Pitzera and F. Glorius, *Chem. Soc. Rev.*, 2018, **47**, 7190–7202.
102 X. Zhang, L. Liu, W. Li, C. Wang, J. Wang, W.-H. Fang and X. Chen, *JACS Au*, 2023, **3**, 1452–1463.
103 G. Ma, C. Chen, S. Talukdar, X. Zhao, C. Lei and H. Gong, *Chem. Commun.*, 2020, **56**, 10219–10222.
104 Y.-Q. Miao, Q.-J. Pan, J.-X. Kang, X. Dai, Z. Liu and X. Chen, *Org. Chem. Front.*, 2024, **11**, 1462–1468.
105 M. Liu, W.-M. Cheng, Z.-L. Li, H. Jiang and J. Ma, *Green Chem.*, 2025, **27**, 3634–3639.
106 T. L. Cheung and H. Lyu, *ChemElectroChem*, 2025, **12**, e202400560.
107 J. Hong, Q. Liu, F. Li, G. Bai, G. Liu, M. Li, O. S. Nayal, X. Fu and F. Mo, *Chin. J. Chem.*, 2019, **37**, 347–351.
108 J.-J. Dai, X.-X. Teng, W. Fang, J. Xu and H.-J. Xu, *Chin. Chem. Lett.*, 2022, **33**, 1555–1558.
109 L. M. Barton, L. Chen, D. G. Blackmond and P. S. Baran, *Proc. Natl. Acad. Sci. U. S. A.*, 2021, **118**, e2109408118.
110 B. Wang, P. Peng, W. Ma, Z. Liu, C. Huang, Y. Cao, P. Hu, X. Qi and Q. Lu, *J. Am. Chem. Soc.*, 2021, **143**, 12985–12991.
111 X. Kong, L. Lin, Q. Chen and B. Xu, *Org. Chem. Front.*, 2021, **8**, 702–707.
112 M. Aelterman, P. Jubault and T. Poisson, *Eur. J. Org Chem.*, 2023, **26**, e202300063.
113 Y. Lai, A. Halder, J. Kim, T. J. Hicks and P. J. Milner, *Angew. Chem.*, 2023, **135**, e202310246.
114 X. Zeng, *Chem.–Eur. J.*, 2024, **30**, e202402220.
115 C. Kingston, M. D. Palkowitz, Y. Takahira, J. C. Vantourout, B. K. Peters, Y. Kawamata and P. S. Baran, *Acc. Chem. Res.*, 2020, **53**, 72–83.
116 A. R. M. Salah, *Electrochemical Organic Synthesis: Mechanistic and Environmental Perspectives*, Shorouk Academy, Cairo, 2025.

117 H. Sheng, J. Sun, O. Rodríguez, B. B. Hoar, W. Zhang, D. Xiang, T. Tang, A. Hazra, D. S. Min, A. G. Doyle, M. S. Sigman, C. Costentin, Q. Gu, J. Rodríguez-López and C. Liu, *Nat. Commun.*, 2024, **15**, 2781.
118 R. Wang, F. Chen, L. Jiang and W. Yi, *Adv. Synth. Catal.*, 2021, **363**, 1904–1911.
119 L. Du, L. Sun and H. Zhang, *Chem. Commun.*, 2022, **58**, 1716–1719.
120 L. Du, B. Zhang, S. Ji, H. Cai and H. Zhang, *Sci. China Chem.*, 2023, **66**, 534–539.
121 W. Guan, Y. Chang and S. Lin, *J. Am. Chem. Soc.*, 2023, **145**, 16966–16972.
122 B. Wang, X. Zhang, Y. Cao, L. Zou, X. Qi and Q. Lu, *Angew. Chem.*, 2023, **135**, e202218179.
123 J. Kuzmin and H. Lundberg, *ChemRxiv*, 2024, preprint, DOI: 10.26434/chemrxiv-2024-9r9hl.
124 H. Shu, X. Tao, S. Ni, J. Liu, J. Xu, Y. Pan and Y. Wang, *Chem. Sci.*, 2025, **16**, 2682–2689.
125 K. Studer, P. Nesvadba, T. Jung, J. Benkhoff, K. Powell and C. Lordelot, *Prog. Org. Coating*, 2008, **61**, 119–125.
126 N. Kvasovsa and V. Gevorgyan, *Chem. Soc. Rev.*, 2021, **50**, 2244–2259.
127 Q. Liu, J. Hong, B. Sun, G. Bai, F. Li, G. Liu, Y. Yang and F. Mo, *Org. Lett.*, 2019, **21**, 6597–6602.
128 Y. Ma, Y. Pang, S. Chabbra, E. J. Reijerse, A. Schnegg, J. Niski, M. Leutzsch and J. Cornella, *Chem.–Eur. J.*, 2020, **26**, 3738–3743.
129 A. Székely and M. Klussmann, *Chem.–Asian J.*, 2019, **14**, 105–115.
130 M. Huang, J. Hu, I. Krummenacher, A. Friedrich, H. Braunschweig, S. A. Westcott, U. Radius and T. B. Marder, *Chem.–Eur. J.*, 2022, **28**, e202103866.
131 T.-Y. Peng, F.-L. Zhang and Y.-F. Wang, *Acc. Chem. Res.*, 2023, **56**, 169–186.
132 P. Nguyen, C. Dai, N. J. Taylor, W. P. Power, T. B. Marder, N. L. Pickett and N. C. Norman, *Inorg. Chem.*, 1995, **34**, 4290–4291.
133 B. Sun, S. Zheng and F. Mo, *Chem. Commun.*, 2021, **57**, 5674–5677.
134 Y. Yamamoto, Y. Konakazawa, K. Fujiwara and A. Ogawa, *Beilstein J. Org. Chem.*, 2024, **20**, 2577–2584.
135 K. Takahashi, S. J. Geib, K. Maeda, D. P. Curran and T. Taniguchi, *Org. Lett.*, 2021, **23**, 1071–1075.
136 P.-F. Zhong, J.-L. Tu, Y. Zhao, N. Zhong, C. Yang, L. Guo and W. Xia, *Nat. Commun.*, 2023, **14**, 6530.
137 X. Yang, H. Wang, Y. Zhang, W. Su and J. Yu, *Green Chem.*, 2022, **24**, 4557–4565.
138 J. R. Montero Bastidas, A. Yadav, S. Lee, B. Ghaffari, M. R. Smith and R. E. Maleczka, Jr, *Org. Lett.*, 2024, **26**, 5420–5424.
139 J. F. Hartwig, *Chem. Soc. Rev.*, 2011, **40**, 1992–2002.
140 Y. Guo, M. Wang and G. Liu, *Asian J. Org. Chem.*, 2024, **13**, e202400464.
141 G. Li, G. Huang, R. Sun, D. P. Curran and W. Dai, *Org. Lett.*, 2021, **23**, 4353–4357.
142 S.-C. Ren, F.-L. Zhang, A.-Q. Xu, Y. Yang, M. Zheng, X. Zhou, Y. Fu and Y.-F. Wang, *Nat. Commun.*, 2019, **10**, 1934.
143 M. Kohansal, *Int. J. New Chem.*, 2025, **12**, 726–737.
144 S. Sharma, F. Gallou and S. Handa, *Green Chem.*, 2024, **26**, 6289–6317.
145 C. Tu, N. Ma, Q. Xu, W. Guo, L. Zhou and G. Zhang, *Int. J. Quantum Chem.*, 2022, **122**, e26920.
146 N. Ma, Q. Wang, D. Zhao, B. Duan, S. Li and G. Zhang, *Org. Chem. Front.*, 2025, **12**, 3163–3176.
147 J. F. Reynes, F. Leon and F. García, *ACS Org. Inorg. Au*, 2024, **4**, 432–470.
148 V. Blay, B. Tolani, S. P. Ho and M. R. Arkin, *Drug Discov. Today*, 2020, **25**, 1807–1821.
149 G. Lyall-Brookes, A. C. Padghama and A. G. Slater, *Digital Discovery*, 2025, **4**, 2364–2400.
150 Y.-F. Shi, Z.-X. Yang, S. Ma, P.-L. Kang, C. Shang, P. Hu and Z.-P. Liu, *Engineering*, 2023, **27**, 70–83.